What is there to gain and lose from plant-derived nano-enabled pesticides: eugenol-loaded nanocarriers exert long-lived effects on non-target freshwater invertebrate communities

Nederstigt, T.A.P.; Huijer, V.N.; Planjer, D.; Eekhout, F.J.M.; Barmentlo, S.H.; Peijnenburg, W.J.G.M.; Vijver, M.G.

Journal of Hazardous Materials 496 (2025) 139560

Contents lists available at ScienceDirect

Journal of Hazardous Materials

journal homepage: www.elsevier.com/locate/jhazmat

What is there to gain and lose from plant-derived nano-enabled pesticides: Eugenol-loaded nanocarriers exert long-lived effects on non-target freshwater invertebrate communities

Tom A.P. Nederstigt [a,*], Victor N. Huijer [a], Dennis Planjer [a], Felice J.M. Eekhout [a], S. Henrik Barmentlo [a], Willie J.G.M. Peijnenburg [a,b], Martina G. Vijver [a]

[a] Institute of Environmental Sciences, Leiden University, Leiden, The Netherlands
[b] Center for Safety of Substances and Products, National Institute for Public Health and the Environment, Bilthoven, The Netherlands

HIGHLIGHTS

- Application of eugenol at nominal concentrations of 20 and 200 μg L^{-1} affected all groups of invertebrates.
- Freely dissolved eugenol concentrations in mesocosms decreased to below the limit of detection within 48 h.
- Effects were characterized by persistent losses in abundances across taxa.
- The nanocarrier-based eugenol formulation exacerbated and extended overall impacts.

GRAPHICAL ABSTRACT

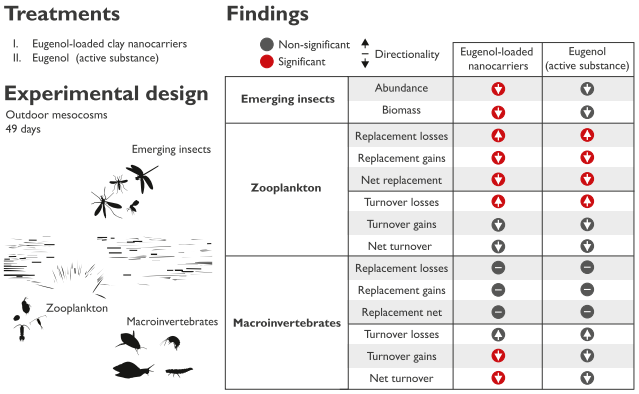

ARTICLE INFO

Keywords:
Nano-pesticide
Advanced materials
Controlled-release
Mesocosm
Biodiversity

ABSTRACT

Nanocarriers are attracting growing interest as transport and delivery systems for agrochemicals. Non-target effects associated with their use have however remained characterized to only a limited extent. The current study comprised a long-term impact assessment of eugenol-loaded clay nanocarriers on naturally established communities of freshwater macroinvertebrates, zooplankton, and emerging insects. Assessments took place in outdoor mesocosms to which eugenol was applied at nominal concentrations of 20 and 200 μg L^{-1}, and effects from the nanocarrier-based formulation were evaluated at concentrations equivalent to those from its active substance. Both concentrations of eugenol adversely affected turnover, replacement, and emergence rates across various taxa, and effects were most pronounced and long-lived when eugenol was applied via the nanocarrier-based formulation. Effects on zooplankton communities and insect emergence rates persisted throughout the 49-day experimental period, while effects on macroinvertebrate communities were limited to the first 7 days following treatment application. These findings underscore the need for further evaluations of exposure

* Corresponding author.
E-mail address: t.a.p.nederstigt@cml.leidenuniv.nl (T.A.P. Nederstigt).

https://doi.org/10.1016/j.jhazmat.2025.139560
Received 2 July 2025; Received in revised form 25 July 2025; Accepted 12 August 2025
Available online 13 August 2025

pathways of nanocarrier-bound substances, and in addition highlight the importance of comparative assessments of non-target impacts from nanocarrier-based formulations with those of their active substance.

1. Introduction

The development of nanocarrier-based products and formulations has made notable headway across various industries over the past two decades. Applications in medicine and cosmetics, where nanocarriers are now routinely used to improve the stability of formulations, optimize the bioavailability of active substances, and enable targeted delivery within the human body, have already received clinical approval several years ago [1,2]. Despite a growing interest in similar applications of nanocarriers for pesticides and fertilizers, only a handful of nanocarrier-based agrochemicals have reached the market and are currently in use in agricultural practices worldwide [3–5]. A scarcity of representative data on potential modulating effects from nanocarriers on the fate and non-target toxicity of active substances, particularly from longer-term studies focusing on higher levels of ecological organization (i.e., populations and communities), has been noted as a key barrier in this regard [3,6,7].

As recently outlined by Gressler et al. [8], nanocarriers represent a diverse class of materials that vary in terms of composition, ranging from organic polymers and lipids to inorganic clays and hybrid materials, as well as in functional attributes. Functional attributes of nanocarriers by definition relate to their ability to incorporate, protect, and deliver active substances, which separates nanocarriers from conventional (or first-generation) nanomaterials and places them within the emerging class of Advanced Materials (AdMa), i.e., materials that are rationally designed to have new or enhanced properties and structural features with the objective of achieving specific or improved functional performance [9]. In contrast to conventional nanomaterials, the current working definition of nanocarriers furthermore encompasses materials that exceed physical dimensions of 100 nm, including carrier systems measuring up to 1000 nm, and sometimes even several micrometers in size [8,10].

Similar to their use in medicine, nanocarriers have been suggested to offer strategic solutions to commonly encountered limitations of active substances in pesticide formulations [4,11]. These limitations include high hydrophobicity, volatility, and sensitivity to environmental degradation, properties which can render substances that otherwise exhibit suitable pesticidal activity unfit for use in pest control [8]. Notable examples of compounds exhibiting such properties are plant-derived essential oils (EOs) and phenolic compounds, which are gaining increasing interest as alternatives to synthetic pesticides in both organic and conventional agricultural practices [12–14]. By encapsulating or binding such substances, nanocarriers can enhance their dispersion in aqueous environments, prolong their stability under field conditions, and allow for a more targeted delivery to pest organisms or specific environmental and biological compartments of interest [15,16]. Products developed using this strategy are commonly referred to as controlled-release formulations, and a growing body of research also supports their application to synthetic active substances currently authorized for use in conventional agricultural practices [17–19].

While it has been suggested that functionalities such as those described above could improve the overall efficacy of active substances, reduce required application rates, and mitigate undesired impacts on non-target organisms, actual experimental validation of such claims remains sparse [3,20]. Moreover, several functionalities of nanocarriers aimed at improving target-toxicity have been noted to also exhibit potential to exacerbate toxicity to non-target organisms, e.g., by altering fate and exposure dynamics of carrier-bound active substances, or by enhancing bioavailability as a result of increased adsorption to biological surfaces, or absorption across biological barriers [21,22]. Given that nanocarrier-based pesticides are generally intended to be applied in close vicinity of (natural) ecosystems, potential collateral impacts on non-target organisms upon translocation to soils, groundwaters, and surface waters through e.g., spray drift and runoff may be considered a crucial aspect in weighing their favorability over conventional pesticide products [21,23]. To this end, there remains a notable lack of data from comparative studies that explicitly evaluate non-target impacts from novel, carrier-based formulations in parallel with their active substances, as well as from higher-tier, environmentally realistic experimental designs that capture relevant fate dynamics and the potential propagation of toxicity to community-level impacts [3,20,24–26].

The current study aimed to (1) experimentally assess impacts of clove (*Syzygium aromaticum*) essential oil-loaded clay nanocarriers on communities of freshwater macroinvertebrates, zooplankton, and emerging insects, and (2) determine the extent to which the nanocarrier-based formulation modulates potential impacts from its active substance, i.e., eugenol. Eugenol is the primary constituent of essential oils derived from *S. aromaticum* flower buds and exhibits pesticidal activity against a variety of agriculturally relevant pest species [14,27–29]. In the European Union, eugenol is currently approved as an active substance in plant protection products for both conventional and organic farming [30,31]. Nanocarriers were composed of sepiolite, a naturally abundant magnesium silicate characterized by a high surface area-to-volume ratio due to its fibrous morphology and open channel (tunnel-like) structure. These structural features, together with the presence of surface hydroxyl groups, magnesium sites, and silanol groups, contribute to sepiolite's high adsorption capacity, making it an attractive and cost-effective carrier material for applications in pesticide formulations [32–36].

Impacts from the nanocarrier-based formulation and eugenol were assessed in parallel at equivalent concentrations of the latter (i.e., 20 and 200 μg L^{-1}) by means of a long-term (i.e., 49-day) outdoor mesocosm experiment, focusing on community dynamics of macroinvertebrates, zooplankton, and emerging insects. By offering direct comparisons between impacts from the nanocarrier-based formulation and those of its active substance, the current work provides an illustrative example of how higher-tier ecotoxicological assessments can be tailored to suit the evaluation of nanocarrier-based products and formulations.

2. Materials and methods

2.1. Test location and experimental setup

The experiment took place between May and September 2023 at the 'Living Lab', an outdoor ecological research facility located in Leiden, the Netherlands (see SI Figure 1 for a visual impression). The Living Lab consists of a parallel series of freshwater mesocosms (length-width-depth: 6 × 0.8 × 0.3 m; approximate volume: 1440 L), which were constructed with minimal use of artificial substrates and mimic typical characteristics of agricultural drainage ditches. Four months before the first sampling moment, each mesocosm was inoculated with a homogenized layer of sediment of approximately 2 cm, collected from nearby waterbodies to promote the establishment of microbes, macrophytes, phytoplankton, zooplankton, and macroinvertebrates. Mesocosms were subsequently connected to an adjacent canal, fed by a branch of the river Rhine, which along with colonization via land and air, facilitated further ecological development. To prevent the entry of vertebrates and other large organisms, a mesh barrier with a 1 cm mesh size was installed at each canal connection. One month before the first sampling, mesocosms were hydrologically isolated from the adjacent canal by placement of stainless-steel barriers and left to equilibrate. All mesocosms remained isolated from surrounding waters for the duration of the experiment to

prevent the exchange of biota and treatments with surrounding waters, and barriers were not removed until measured concentrations of the applied treatments were below detection limits. Physicochemical water quality parameters (i.e., temperature, pH, dissolved oxygen conductivity, chlorophyll A, and turbidity) were measured weekly throughout the experiment, starting two weeks before treatment application, using a Hach HQ40d multimeter (Hach Ltd., Colorado, USA) and a AquaFluor® handheld fluorometer (Turner Designs, Inc., San Jose, USA), and are reported in SI Figure 2.

2.2. Treatments and characterization

Treatments consisted of (1) clove essential oil (CEO)- loaded sepiolite nanocarriers, of which eugenol was considered the active substance, and (2) eugenol in freely dissolved form. Both formulations were applied according to equivalent concentrations of eugenol (i.e., 20 and 200 μg L^{-1}) to enable direct comparisons of their potential effects. Eugenol was obtained from Sigma-Aldrich (99 % purity, Massachusetts, USA), and CEO-loaded nanocarriers were provided by Encapsulae SL (Castellón de la Plana, Spain). CEO-loaded nanocarriers consisted of clove essential oil adsorbed to layered and fibrillar sepiolite (magnesium silicate) nanoclay particles (7–8 % w/w), and the clove oil used in the production of CEO-loaded nanocarriers contained eugenol (84 % v/v), caryophyllene (16 % v/v) and carvacrol (0.02 % v/v). CEO-loaded nanocarriers were encapsulated with 2–3 % wt/wt fumaric acid, which is sparingly soluble in water (7.3×10^{-3} mg L^{-1}), and thereby retards the release of encapsulated substances in aqueous media [37]. Analysis of methanol extracts from the CEO-loaded nanocarriers by gas chromatography coupled to mass spectrometry (GC-MS) yielded relative concentrations of eugenol and caryophyllene of 99.97 % and 0.03 %, respectively, and as such, eugenol was considered the sole active substance of interest in the current study. Hereafter, the nanocarriers used in the current study are therefore referred to as eugenol-loaded. A comprehensive description of the production process of the eugenol-loaded nanocarriers has previously been reported in Brinkmann et al. [38] and Pizzol et al. [39].

Treatment concentrations were selected based on available ecotoxicity data for eugenol, with the aim of detecting moderate long-term effects, thereby enabling the assessment of potential differences in impacts between the nanocarrier-based formulation and its active ingredient. While available ecotoxicity data suggest low acute toxicity of eugenol to freshwater invertebrates (reported 50 %-effect concentrations from *Daphnia magna* immobilization tests ranging from 0.14 to 1.13 mg L^{-1}), longer-term toxicity data from experimental assays are currently lacking [38,40,41]. The highest test concentration (200 μg L^{-1}) applied in the current experiment was therefore derived by applying an acute-to-chronic ratio of ~6 to highest reported acute EC_{50} for *D. magna* [41]. To achieve target eugenol concentrations of 20 and 200 μg L^{-1}, corresponding sepiolite concentrations in nanocarrier treatments were 317 and 3170 μg L^{-1}, respectively. There is currently no toxicity data available for sepiolite clay in freshwater organisms. However, experiments with *D. magna* have yielded no-observed-effect concentrations (NOECs) and lowest-observed-effect concentrations (LOECs) for other natural clays that typically exceed the concentrations of sepiolite used in the present study by several orders of magnitude [42,43]. Based on this, it was assumed that direct toxicity from sepiolite in the nanocarrier treatments would be negligible.

The morphology of bare and eugenol-loaded nanocarriers was characterized using Transmission Electron Microscopy (TEM, JEOL 1010, JEOL Ltd., Tokyo, Japan), and lengths, widths, and aspect ratios were measured from TEM micrographs using ImageJ (ver. 1.53a [44]). Hydrodynamic diameters, polydispersity indices (PDIs), sedimentation rates (based on derived count rates, which reflect the intensity of scattered light and decrease as particles settle out of suspension), and ζ-potential of eugenol-loaded nanocarriers were assessed over time in water derived from the experimental site using a Malvern Zetasizer Ultra (Malvern, Malvern, UK). Hydrodynamic diameters, PDIs, sedimentation rates, and ζ-potential were assessed only at the highest treatment concentration (200 μg L^{-1} eugenol), since pilot tests at the lower treatment concentration (20 μg L^{-1} eugenol) yielded results that were considered insufficiently robust. Water from the experimental site was pre-filtered over 0.45 μm cellulose filters (Millipore, Massachusetts, USA) prior to preparation of test suspensions. Measurements of hydrodynamic diameters and PDIs were obtained from samples ($n = 5$) that were left unagitated, and measurements were continued at regular intervals (one, two, three, five, seven and 24 h after preparation, and subsequently at 24 h intervals) until obtained signals could not be distinguished from background noise (i.e., from naturally occurring suspended matter that passed the pre-filtering step).

2.3. Treatment application and analyses in the experimental setup

Treatments were administered as single-dose additions to 30 mesocosms (i.e., $n = 6$ per treatment, including controls), arranged according to a systematic block design. Free-eugenol stock solutions were prepared in ethanol (96 % purity; 50/50 v/v) to promote solubility (ethanol concentrations in mesocosms < 0.0001 %). Stock suspensions of eugenol-loaded nanocarriers were prepared in demineralized water to prevent premature desorption of eugenol from the nanocarriers, and stirred at 1300 rpm for one hour prior to application. To ensure that treatments were applied homogeneously to each mesocosm, aliquots from stocks were mixed with 10 L of water collected from receiving mesocosms, which was subsequently reapplied evenly across the surface of each mesocosm using watering cans fitted with perforated caps.

Water samples were collected at one and 24 h, three days, and every subsequent week after treatment application, and stored at −20 °C until processing for quantification of eugenol concentrations. Water samples were centrifuged for 30 min at 14,000 rpm before analysis to remove suspended particles, and as such, measurements of eugenol in water samples from mesocosms that received eugenol-loaded nanocarriers reflected concentrations of dissolved (i.e., desorbed from the nanocarrier) eugenol. Eugenol concentrations in water samples were determined by liquid chromatography-tandem mass spectrometry (LC-MS/MS) on a Waters Aquity I-class FTN system (fitted with a Waters Aquity BEH C18 column, Waters Ltd., Massachusetts, USA) coupled to a ScieX Qtrap 6500 mass spectrometer (ScieX Ltd., Massachusetts, USA). Calibration (0–200 μg L^{-1}) was performed prior to the measurement of each batch of samples using a eugenol standard (PESTANAL® analytical standard, Sigma-Aldrich, Massachusetts, USA). The (lower) limits of detection and quantification (LoD and LoQ) were calculated as 3.3σ/S and 10σ/S (with σ denoting the standard deviation from six matrix control replicates, and S denoting the slope of the calibration curve), and determined at 1.06 (LoD) and 2.17 μg L^{-1} (LoQ), respectively. All samples were measured in duplicate and eugenol-d_3 (99.8 % purity, MCE®, New Jersey, USA) was added as an internal standard at a concentration of 50 μg L^{-1} to each sample.

2.4. Macroinvertebrate and zooplankton community sampling

Macroinvertebrate and zooplankton communities were sampled 14 days prior, and seven, 28, and 49 days after treatment application. For macroinvertebrates, sample volumes were standardized across replicates and time points by isolating 60 cm segments (measured in length, and across the entire width of each mesocosm, totaling to a volume of approximately 140 L) from each mesocosm by forcing stainless steel barriers into the sediment layer before sampling. Macroinvertebrates present on the water surface were collected using featherweight entomological forceps. The water column of the isolated sections was sampled for pelagic macroinvertebrates using a dip net with a mesh size of 150 μm, and sampling was continued until additional dip net sweeps yielded no more specimens. The upper 3–5 cm of sediment of each isolated section was sieved over a 500 μm stainless steel sieve to retrieve

benthic macroinvertebrates. All specimens were identified to the lowest possible taxonomic level (using an in-house identification guide) and counted, and subsequently returned alive to their respective mesocosms within one to two hours. Highly abundant taxa were subsampled from homogenized material, and resulting counts were back-transformed to represent total sample volumes.

Zooplankton were collected from depth-integrated water samples collected from locations spread evenly across the length and width of each mesocosm, totaling to a sample volume of 1 L of per replicate. Samples were concentrated using a zooplankton collection net with a filter mesh size of 53 µm (EFE & GB Nets, Cornwall UK), preserved in a 1 % solution of Lugol's iodine (Sigma Aldrich, Missouri USA), and stored at 4 °C until processing. Specimens were identified and counted from 2 mL aliquots (equivalent to 20 % of the volume of non-concentrated water samples) per homogenized sample using a Zeiss ID 02 inverted microscope (Carl Zeiss AG, Oberkochen, Germany) at 32 × to 200 × magnification. Identification was performed to the lowest possible taxonomic clade feasible (using Floßner [45] and Notenboom-Ram [46], and an in-house identification guide), and abundances were back-transformed to be representative of densities in 1 L of water in the experimental setup prior to further analyses.

2.5. Emerging insect sampling

Emerging insects were continuously sampled from the mesocosms from eight days before to 45 days after treatment application. Emergence traps consisted of stainless-steel pyramid-shaped frames (60 × 60 × 74 cm) covered with No-See-Um mesh netting (300 holes/cm^2). Traps were positioned 5 cm below the water surface by securing them to the banks of the mesocosm using steel pegs, effectively preventing the escape of emerging specimens. Specimens were collected using a capturing system (adapted from Cadmus et al. [47], according to Barmentlo et al. [48]) comprised of two 500 mL polyethylene bottles joined at the caps (with a 3.5 cm opening) and sealed with adhesive. The upper (capture) bottle was connected to the trap via a 5 × 7 cm opening in both the netting and bottle, while the lower (collection) bottle contained 100 mL of 80 % ethanol (diluted in tap water) as a preservative medium. Collection bottles were emptied and replaced two times per week until 35 days after the application of the treatments, and once per week thereafter. Captured specimens were transferred to 25 mL glass snap-cap vials and preserved in 80 % ethanol until identification and quantification using a Zeiss Stemi stereo microscope (Carl Zeiss AG, Oberkochen, Germany). All specimens were identified to Order level, and Dipterans were identified to Family level according to Oosterbroek [49].

Abundances of emerging insects from major Orders (Diptera, Coleoptera, Ephemeroptera, Hemiptera, Hymenoptera, and Odonata) were converted to biomass using gravimetrically derived mean values per taxon published previously in Barmentlo et al. [48]. The current study was conducted in close vicinity of the latter, followed a comparable experimental approach, and samples showed overall similarity in terms of taxonomic composition. Biomass conversions based on values reported in Barmentlo et al. [48] were as such considered sufficiently reliable to allow for comparisons between treatments.

2.6. Data analysis

2.6.1. Particle characterization

Lengths, widths, and aspect ratios of bare and eugenol-loaded nanocarriers derived from TEM micrographs were compared using one-way ANOVAs (function 'anova', R package 'stats'). Rates of change in hydrodynamic diameters, PDIs, and derived count rates (i.e., sedimentation rates) of eugenol-loaded nanocarriers from DLS measurements were estimated from three-parameter exponential decay models (function 'drm', R package 'drc').

2.6.2. Sampling efficacy and pre-treatment homogeneity in community composition

The adequacy of sampling efforts for capturing the diversity of macroinvertebrates, zooplankton, and emerging insects present across mesocosms in the experimental setup was assessed based on the cumulative increase in taxon richness over collected samples (i.e., taxon accumulation curves) before and after treatment application. Sampling was considered sufficiently representative when, on average, fewer than one newly identified taxon was obtained after accounting for one additionally sampled mesocosm. For all time points and groups, this was achieved after fewer than 13 (out of 30) sampled mesocosms (SI Figure 3).

Homogeneity in community composition between mesocosms assigned to different treatments prior to the start of the experiment was assessed based on the overall richness and abundance across taxa for each assessed group, and Bray-Curtis (accounting for differences in abundances across shared taxa) and Sørensen (accounting solely for differences in occurrences, regardless of abundances) dissimilarity for macroinvertebrates and zooplankton [50]. Taxon richness and abundances were compared between mesocosms assigned to different treatments using one-way ANOVAs (function 'anova', R package 'stats') or Kruskal Wallis tests (function 'kruskal.test', R package 'stats'), depending on whether assumptions for parametric models were met, and Bray-Curtis and Sørensen dissimilarity was assessed by Permutational ANOVAs (PERMANOVA, function 'adonis2', R package 'vegan'). For macroinvertebrates, data of Tubificidae were omitted from analyses (both pre- and post-treatment application) due to an overall high abundance in all collected samples and resulting difficulties in reliable quantification.

2.6.3. Richness and abundance

Differences in taxon richness and abundance of macroinvertebrates, zooplankton, and emerging insect communities throughout the experiment were assessed via mixed effect models (function 'lmer', R package 'lme4'). Models included nominally applied eugenol concentrations and time as numerical predictors, and nanocarrier presence as a categorical (i.e., present-absent) predictor. To assess potential interactions between eugenol and the nanocarrier, control data were duplicated to create dummy controls for the nanocarrier treatments, yielding full factorial models under the assumption that nanocarrier effects alone are negligible (see Section 2.2). Models included all interaction terms (i.e., nominal eugenol concentration × nanocarrier presence × time), and random intercepts were fitted for each replicate mesocosm to account for the repeated-measures design. Model fits were compared with those of reduced models in which random effects were omitted according to Akaike's Information Criterion (AICs), and models with the lowest AICs were selected for further inference. False Discovery Rate (FDR) corrected estimated marginal means for pairwise comparisons between concentrations and at time points of interest were derived from models that were refitted with concentration and time as categorical variables (function 'emmeans', R package 'emmeans').

2.6.4. Replacement and turnover in macroinvertebrate and zooplankton communities

Temporal β-diversity indices (TBIs) were calculated to assess replacement and turnover in macroinvertebrate and zooplankton communities over the course of the experiment. In this context, replacement refers to the overall change in community composition over time based on differences in taxon abundance, while turnover refers to changes based solely on differences in taxon presence and absence. TBIs were calculated according to Legendre [51], where the total change in community composition within observational units (i.e., mesocosm) over time ($B + C$) is partitioned into taxon gains (C), losses (B) and net change (C - B). Here, gains per taxon (C_j) denote the fraction of abundance (or incidence) that is higher at the second than at the first time point for a given contrast, and losses (B_j) denote the fraction of the abundance (or

incidence) of a taxon which is higher at the first than at the second time point (SI Equation 1). The summed gains (C) and losses (B) per taxon are subsequently scaled by division by a denominator ($2A + B + C$; with A denoting the summed abundance/incidence per taxon that is shared between time points of interest), resulting in a measure of dissimilarity ranging between from 0 (no change) to 1 (maximum change). TBIs were calculated by contrasting community composition at respective sampling time points after treatment application (i.e., 7, 28, and 49 days) with community composition before treatment application (i.e., −14 days). Replacement was quantified according to the $D_{\%diff}$ index (hereafter Bray-Curtis dissimilarity), and turnover was calculated according to the Sørensen index (function 'TBI', R package 'adespatial'). Taxon-specific gains and losses in abundances and incidences were calculated according to SI Equation 1 in order to provide insights into their contribution to TBI parameters (i.e., community-level gains and losses, and net and total replacement/turnover).

Effects of nominal eugenol concentrations (treated as a numeric predictor) and the nanocarrier (treated as categorical) on gains, losses, net and total replacement/turnover over time were assessed via beta regressions (function 'glmmTMB', R package 'glmmTMB'). Controls were duplicated to generate dummy controls for nanocarrier treatments, yielding full factorial models as described in Section 2.6.3. Nominal eugenol concentrations were rescaled by min-max normalization prior to analyses to facilitate model convergence, and net replacement/turnover was rescaled (originally ranging from −1 to 1) to fall between 0 and 1 to meet requirements for beta regressions. All possible interaction terms were included, and random intercepts were fitted for each replicate mesocosm to account for the repeated-measures design. Model fits were compared with those of reduced models in which random effects were omitted according to Akaike's Information Criterion (AICs), and models with the lowest AICs were selected for further inference. Distributional assumptions for model residuals were assessed using simulation-based diagnostic plots (function 'simulateResiduals', R package 'DHARMa'). Significance of fixed effects was evaluated using Wald χ^2 tests (function 'Anova', R package 'car'), and FDR-corrected estimated marginal means were calculated as stated for the analyses of abundances and richness to derive comparisons between contrasts of interest (Section 2.6.3).

2.6.5. Insect emergence

Abundance data from insects collected in emergence traps were transformed to cumulative counts per mesocosm over time prior to analyses. Data from specimens that were only sporadically present (i.e., Trichoptera and Arachnida) and from those that were small enough to escape through the mesh fitted to the traps (i.e., Collembola and Aphididae), or enter the traps from outside the mesocosms, were omitted from analyses. Data from other orders of insects present in low abundances were pooled, resulting in analyses to be performed separately for Diptera (and therein the families Chironomidae and Ceratopogonidae), and all other orders of insects combined. Generalized additive models (GAMs; function 'gam', R package 'mgcv'), assuming a negative binomial distribution to account for overdispersion, were used to assess the effects of eugenol exposure and its interaction with the nanocarrier on total and taxon-specific emergence. Dummy controls for the nanocarrier treatments were generated as described for the statistical analyses of abundances and richness in Section 2.6.3. First, emergence rates were modelled as a function of nominal eugenol concentrations by including separate smooth terms for concentration for each level of the nanocarrier (present vs. absent), allowing the shape of the concentration response to differ depending on the applied formulation of eugenol (i.e., applied as freely dissolved active substance or via the sepiolite nanocarrier). Second, the interaction between concentration and time was modelled using a tensor product smooth varying by nanocarrier, to assess whether temporal dynamics of effects of eugenol differed depending on the applied formulation. Time was included as a smooth term shared across all treatments using a penalized cubic regression spline with 14 basis functions (reflecting the number of sampling moments), and random intercepts were fitted for each replicate mesocosm using a random effect smoother to account for the repeated-measures design. All smooth terms were penalized to prevent overfitting, and smoothing parameters were estimated via restricted maximum likelihood (REML). Assessment of effects on cumulative insect biomass followed an analogous approach to that of abundances, with the exception that models were fitted assuming a Gaussian distribution with an identity link function. Biomass data were $\log_{10}$-transformed prior to analysis to improve homoskedasticity and model fit.

Data analysis was performed using R version 4.5.0 [52], and outcomes of statistical tests were considered statistically significant at $p < 0.05$.

3. Results and discussion

3.1. Characterization of treatments and exposure conditions in experimental setup

Transmission electron microscopy (TEM) images confirmed that eugenol-loaded sepiolite nanocarriers were fiber-like in shape, with lengths of 918.3 ± 89.8 nm (mean ± standard error, $n = 40$), widths of 32.2 ± 2.0 nm, and an aspect ratio of 31.7 ± 3.4 nm (Fig. 1 a, SI Figure 4). Eugenol-loading did not result in significant alterations of the lengths ($F_{(1,78)} = 0.05$, $p = 0.82$), widths ($F_{(1,78)} = 3.12$, $p = 0.08$), or aspect ratio ($F_{(1,78)} = 3.48$, $p = 0.06$) of the nanocarriers (SI Figure 4). In vitro assessments in water from the experimental site showed that eugenol-loaded nanocarriers exhibited a ζ-potential of −11.8 ± 0.1 mV, and underwent rapid aggregation immediately after preparation of suspensions, resulting in an overall high suspension dispersity (Fig. 1 b & c). Derived count rates from dynamic light scattering (DLS) indicated that the majority of nanocarriers subsequently settled out of suspension within hours after preparation, with an estimated 50 % reduction occurring after 2.6 ± 0.5 h (Fig. 1 d). This coincided with a decrease in hydrodynamic sizes and dispersity indices of the fraction of nanocarriers remaining in suspension, for which 50 % reductions were estimated at 21.0 ± 10.4 and 49.3 ± 17.0 h, respectively. Signals obtained from nanocarriers could be distinguished from background noise (i.e., from naturally occurring suspended matter) until 72 h after preparation of suspensions.

One hour post-application, in situ eugenol concentrations (freely dissolved) were approximately one order of magnitude lower than nominal treatment concentrations, regardless of whether eugenol was applied as freely dissolved active substance or via the nanocarrier-based formulation (Fig. 1 e). Measured concentrations in samples collected at subsequent sampling moments yielded signals below the detection limit for most mesocosms after 24 h, and in all mesocosms at sampling moments thereafter (Fig. 1 f). In natural surface waters, eugenol is expected to adsorb to organic matter (log $K_{ow} = 1.83$), undergo microbial and photodegradation, and to a minor extent volatize from the water surface (estimated Henry's law constant = 1.92×10^{-6} atm·m^3/mol at 25 °C), which has been noted to result in a low persistence in aqueous environment [31,53]. These processes likely contributed to the observed discrepancy between nominal and measured eugenol concentrations, especially considering that mesocosms were relatively shallow, contained natural sediments rich in organic matter, and were situated in sunlit environments.

3.2. Community responses – diversity, temporal replacement, and turnover

3.2.1. Macroinvertebrates

A total of 14,532 macroinvertebrates were collected across all mesocosms over the course of the experiment (SI Figure 5 a). Gastropoda (snails; 9 taxa) were the most abundant class, accounting for 40.1 % of all specimens, followed by Insecta (insects; 38.7 %; 52 taxa).

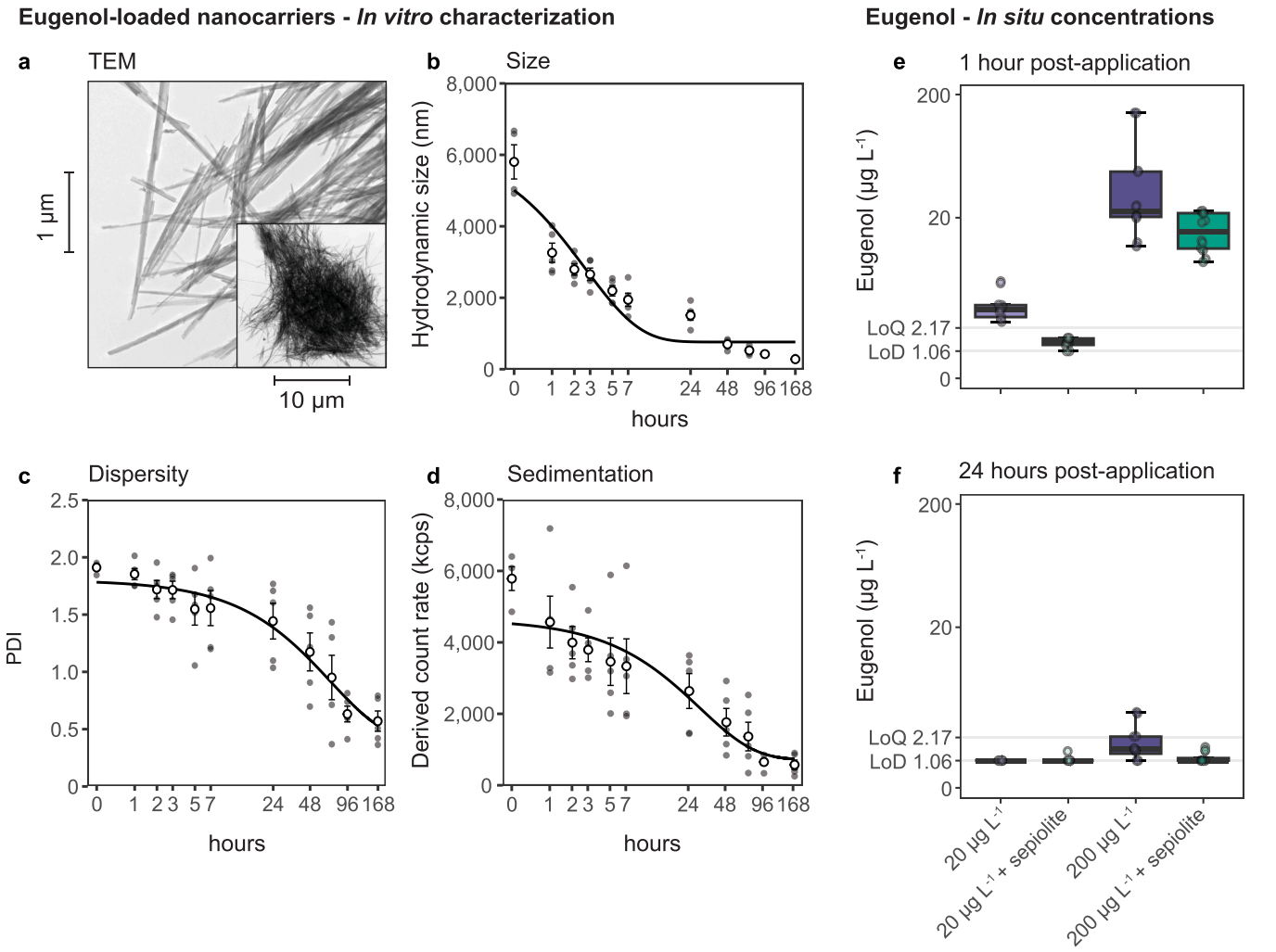

Fig. 1. *In vitro* characterization of eugenol-loaded sepiolite nanocarriers and in situ concentrations of eugenol (active substance) in the experimental setup. **a**: Transmission electron micrographs (TEM) illustrating a fibrillar morphology of the sepiolite nanocarriers (8000 × and 2000 × magnification for main and embedded image, respectively). **b** - **d**: Hydrodynamic diameters, polydispersity indices (PDIs) and estimated sedimentation rates (based on derived count rates) assessed using dynamic light scattering (DLS) at the highest treatment concentration (200 µg L^{-1} + eugenol) in water derived from the experimental site over time (mean ± standard error, $n = 5$). Trend lines are derived from three-parameter exponential decay models. **e** & **f**: Eugenol concentrations (freely dissolved) in the experimental setup one and 24 h post-treatment application. Treatment concentrations reported on the x-axes reflect nominal concentrations of eugenol (applied as freely dissolved active substance or via the sepiolite nanocarrier). LoD and LoQ denote the Limit of Detection and (Lower) Limit of Quantification, calculated as 3.3σ/S and 10σ/S (σ = standard deviation from six matrix control replicates, S = slope of the calibration curve). Lines, boxes, and whiskers denote the median, interquartile range, and 1.5 × the interquartile range, respectively. Water samples collected at two and 10 days post-treatment application consistently yielded signals for eugenol concentrations below the LoD for all treatments ($n = 6$).

Malacostraca (primarily amphipods and isopods; 6 taxa) represented 11.4 % of totals, while Arachnida (exclusively spiders; 3 taxa) made up 6.2 %. Clitellata (oligochaetes and leeches; 8 taxa) contributed 3.6 %, and Bivalvia (mussels) and Entognatha (exclusively *Podura aquatica*) were encountered only sporadically, each representing less than 0.01 % of the total number of collected macroinvertebrates. Prior to treatment application, macroinvertebrate communities showed minor variation and no significant differences between mesocosms assigned to different treatments in terms of abundance ($F_{(4,25)} = 0.92$, $p = 0.47$) and taxon richness ($F_{(4,25)} = 1.06$, $p = 0.40$), with means (± standard error) per sampled segment across all mesocosms being 72.0 ± 8.8 and 9.9 ± 0.5, respectively (SI Figure 6 a & b, SI Table 1). Likewise, macroinvertebrate communities exhibited overall similarity between treatments in abundance- (Bray-Curtis: $F_{(4,25)} = 0.75$, $p = 0.81$) and incidence-based (Sørensen: $F_{(4,25)} = 1.19$, $p = 0.25$) measures of community composition (SI Figure 7 a & e, SI Table 2).

Measures of overall taxon richness (Eugenol: $\chi^2_{(1)} = 1.18$, $p = 0.28$; Eugenol × Time: $\chi^2_{(1)} = 0.05$, $p = 0.82$) and abundance (Eugenol: $\chi^2_{(1)} = 1.72$, $p = 0.19$; Eugenol × Time: $\chi^2_{(1)} = 2.36$, $p = 0.12$) of macroinvertebrates showed no significant differences between treatments and controls at any of the sampling moments, regardless of whether eugenol was applied in its freely dissolved form or via the nanocarrier-based formulation (SI Figure 6 a & b, SI Table 1). Macroinvertebrate communities did however change significantly in richness and abundance over time, with gains in abundances (Bray-Curtis - Time: $\chi^2_{(1)} = 50.0$, $p = 1.5 \times 10^{-12}$) relative to pre-treatment conditions progressively increasing and outweighing losses (Bray-Curtis - Time: $\chi^2_{(1)} = 0.40$, $p = 0.53$), particularly from seven days after application of the treatments onwards (Fig. 2 a & b). A similar, albeit less pronounced predominance of gains (Sørensen - Time: $\chi^2_{(1)} = 4.58$, $p = 0.03$) over losses (Sørensen - Time: $\chi^2_{(1)} = 5.50$, $p = 0.02$) was observed for turnover rates, i.e., incidence-based changes in community composition (Fig. 2 c & d). Here, increasing eugenol concentrations, when applied via the nanocarrier-based formulation, did result in a statistically significant decrease in gained taxa over time (Sørensen - Eugenol × Nanocarrier: $\chi^2_{(1)} = 5.21$, $p = 0.02$). This was primarily driven by fewer newly

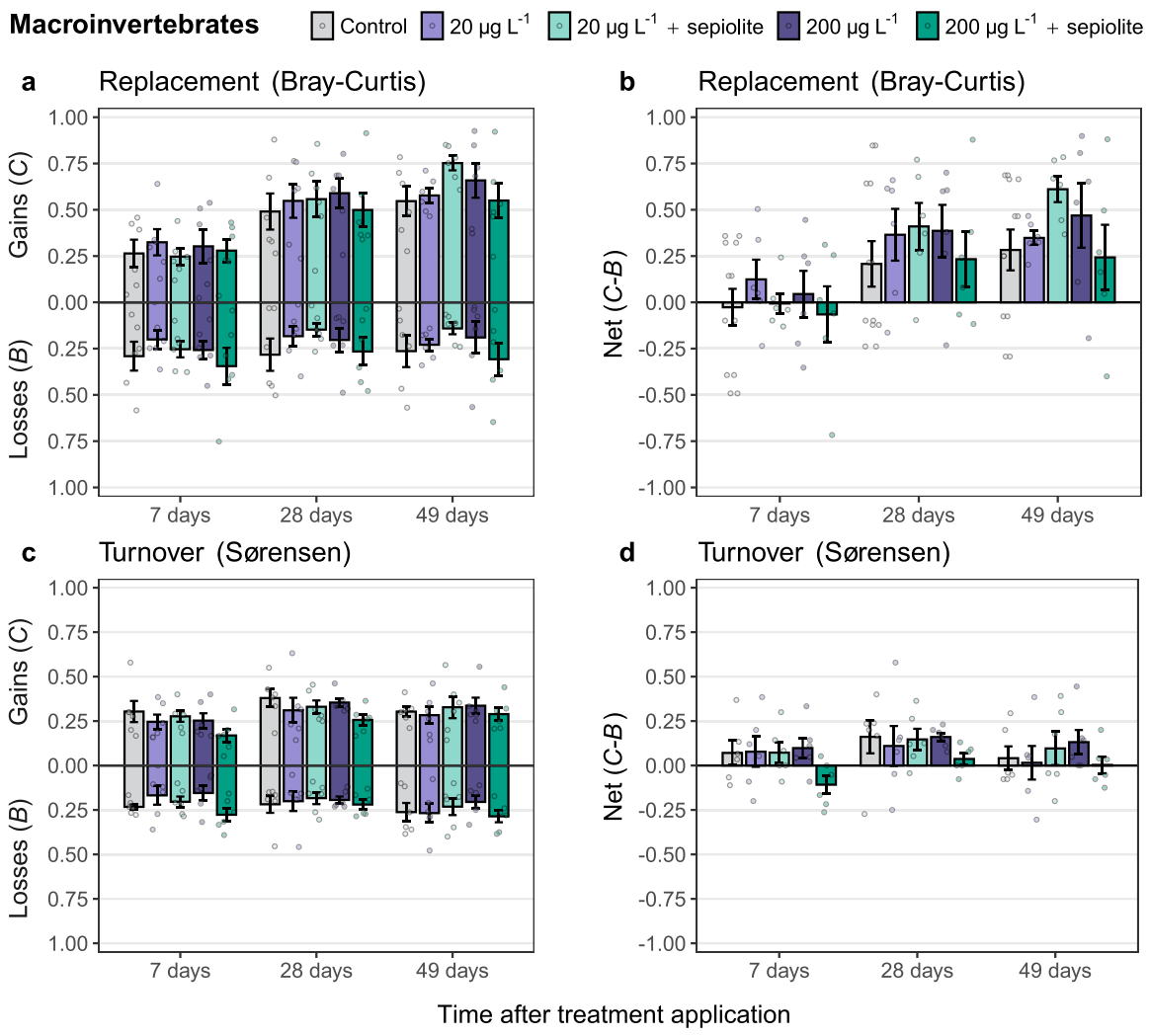

Fig. 2. Temporal replacement (mean ± standard error, $n = 6$) in abundances (**a** & **b**) and turnover (**c** & **d**) of macroinvertebrate communities over the course of the experiment. Treatment concentrations reported in the legend reflect nominal applications of eugenol (applied as freely dissolved active substance or via the sepiolite nanocarrier). Replacement and turnover are expressed as normalized dissimilarity coefficients, indicating the summed and scaled change in abundances/incidence across taxa calculated per replicate, for respective time points relative to pre-treatment conditions (-14 days). Replacement and turnover are decomposed into gains (*C*) and losses (*B*) and scaled from 0 to 1, with 0 denoting no change and 1 denoting maximum change. Net replacement/turnover rates (*C* - *B*) are scaled from −1 to 1, with −1 denoting maximum net negative replacement or turnover (i.e., losses), 0 denoting no net replacement or turnover (i.e., losses equaling gains), and 1 denoting maximum net positive replacement or turnover (i.e., gains). See SI Table 3 for the full output of statistical tests.

observed taxa at the 200 µg L^{-1} treatment concentration seven days after its application (odds ratio = 2.15 ± 0.63 standard error, Z = 2.60, $p = 0.03$), with gains being 44.3 ± 14.9 % lower than in controls, and 33.1 ± 15.5 % lower than in mesocosms where equivalent concentrations were applied as freely dissolved active substance (mean ± propagated standard error). Together with slightly more pronounced losses than observed in controls (19.0 ± 5.4 %), this resulted in net negative turnover rates in the 200 µg L^{-1} nanocarrier treatments, while macroinvertebrates in controls and all other treatments at this sampling moment showed net positive turnover rates (odds ratio = 1.43 ± 0.27 standard error, Z = 1.89, $p = 0.09$).

Overall, observations from turnover rates suggest that macroinvertebrate communities were most affected by eugenol when applied via the nanocarrier-based formulation. It should however be noted that differences from controls in this regard were (1) only observed at the 200 µg L^{-1} treatment concentration, (2) relatively small compared to the overall variation observed across treatments and controls, and (3) short-lived, as illustrated by a reduced magnitude at subsequent sampling moments (Fig. 2 a & b). Further analyses of taxon-specific contributions illustrated that rates of replacement in macroinvertebrate communities were driven largely by shifts in abundances of only a small number of taxa (Fig. 3). Differences from controls in this regard were most pronounced for *Gammarus pulex*, which after seven days had temporarily decreased in abundance in response to the highest treatment concentration, with declines being most prominent in mesocosms where eugenol was applied via the nanocarrier-based formulation. Taxon-specific rates of turnover in contrast showed that gains and losses in incidence of macroinvertebrates were the product of more subtle temporal changes across a larger number of taxa, most of which exhibited a lower occupancy across replicates in the experimental setup (SI Figure 9). In correspondence, differences in overall turnover rates from controls in the 200 µg L^{-1} nanocarrier treatments could be attributed to relatively minor shifts in incidences across various taxa, with Malacostraca being the only phylum within which taxa consistently showed either a net negative (i.e., *Asellus aquaticus*, *Proasellus coxalis*, *Gammarus pulex*, and *Orconectus limosus*) or net neutral (*Gammarus tigrinus* and *Procambarus clarkii*) difference from controls.

3.2.2. Zooplankton

Zooplankton communities (111,816 specimens, back-transformed to

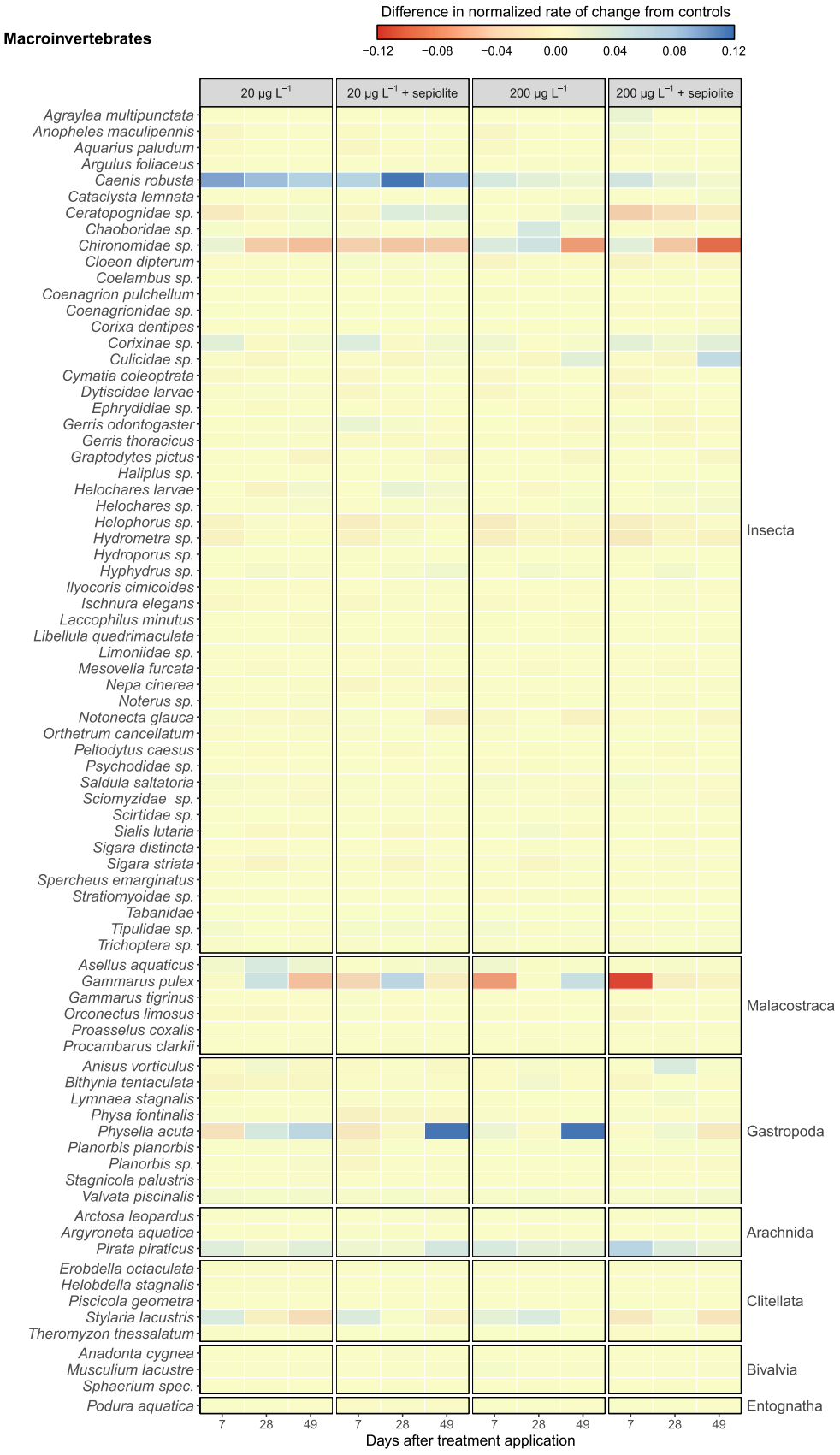

(caption on next page)

Fig. 3. Differences between treatments and controls in (mean) normalized rates of change in abundances of macroinvertebrates over the course of the experiment. Treatment concentrations reflect nominal applications of eugenol (applied as freely dissolved active substance or via the sepiolite nanocarrier). Differences between treatments and controls are calculated based on the normalized net change in abundance (calculated per replicate) between respective time points and pre-treatment conditions (-14 days), which in turn is directly proportional to the contributions of individual taxa to temporal replacement in abundances at the community level (see Fig. 2 **a** & **b**). Positive differences in rates of change for a given treatment and time contrast denote that abundances of a taxon on average either increased more, or decreased less than in controls. Negative differences in rates of change in turn denote that abundances of a taxon either increased less, or decreased more than in controls. The limits of the color scale are adjusted to the minimum and maximum observed difference in rates of change across all comparisons, and winsorized at ± 0.12 to improve contrast. Only values for *Physella acuta* at 49 days post treatment application exceeded this threshold. Taxa are clustered by Phylum, i.e., Insecta (insects), Malacostraca/Crustacea (crustaceans), Gastropoda (gastropods), Archnida (exclusively spiders), Clitellata (clitellate annelid worms), Bivalvia (bivalves), and Entognatha/Collembola (water springtails). An equivalent overview based on presence-absence data (i.e., contributions to turnover rates) is provided in SI Figure 9.

abundances L^{-1}) showed a dominance of Copepoda (65.3 % of all specimens), which could largely be attributed to high abundances of juvenile individuals (i.e., Nauplii; 59.6 %) (SI Figure 5 b). Adult Copepoda (including Calanoida and Cyclopoida) were comparatively less abundant (5.7 %). Rotifera represented the second most abundant group of zooplankton (12.5 %; 18 taxa), followed closely by Ostracoda (11.2 %; 1 taxon) and Cladocera (11.1 %; 6 taxa). Zooplankton communities showed no significant differences between mesocosms assigned to different treatments prior to their application in overall abundance ($F_{(4,25)} = 1.02$, $p = 0.42$) and taxon richness ($F_{(4,25)} = 1.52$, $p = 0.23$), with respective means (± standard error) per liter across all mesocosms of 1251 ± 164 and 7.0 ± 0.3 (SI Figure 6c & d, SI Table 1). Likewise, zooplankton communities exhibited no significant dissimilarity in terms of abundance- (Bray-Curtis: $F_{(4,25)} = 1.22$, $p = 0.30$) or incidence-based (Sørensen: $F_{(4,25)} = 1.07$, $p = 0.42$) measures of community composition (SI Figure 8 a & e, SI Table 2).

Zooplankton communities in mesocosms that received the highest treatment concentrations of eugenol (i.e., 200 µg L^{-1}) exhibited slight

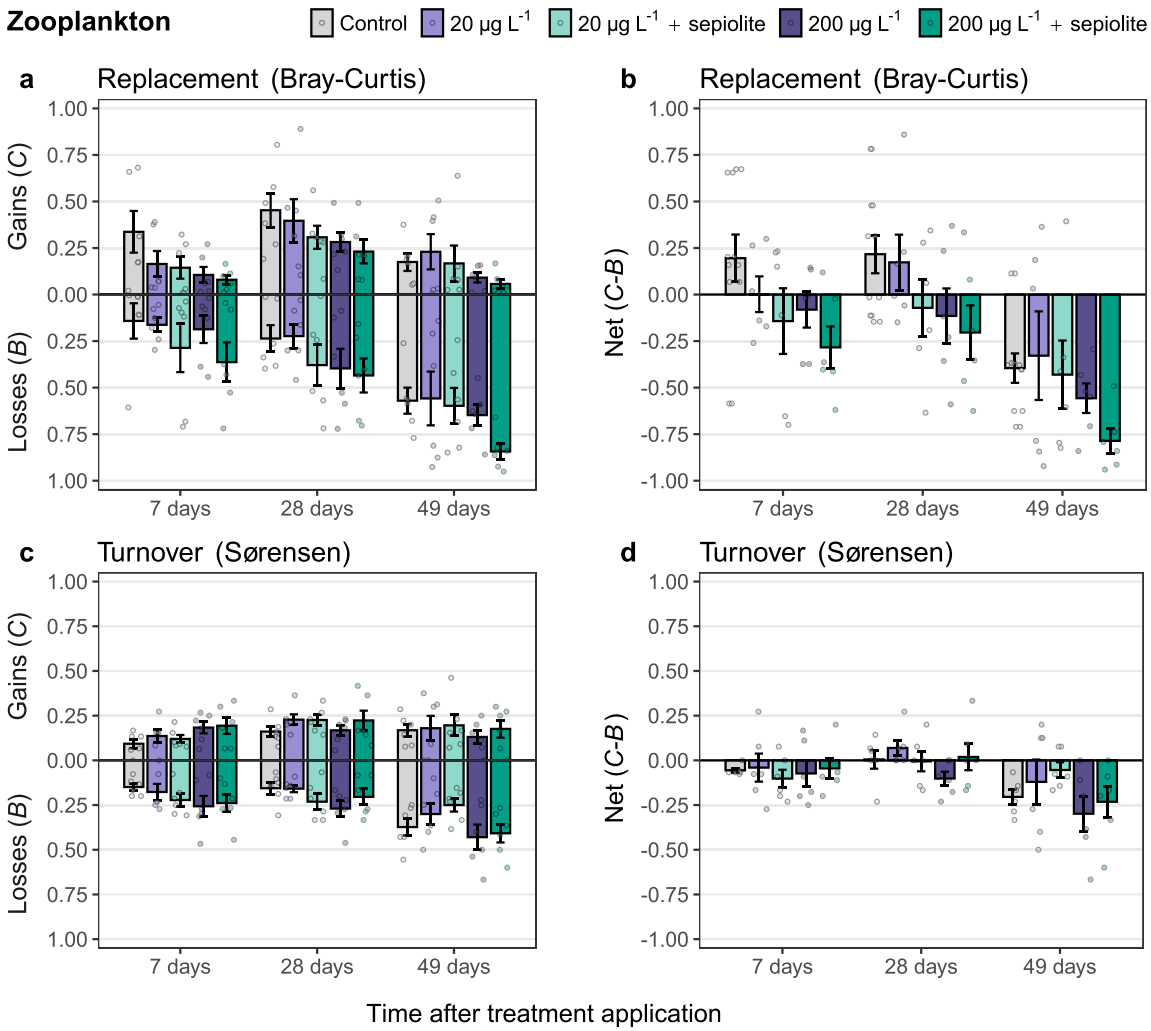

Fig. 4. Temporal replacement (mean ± standard error, $n = 6$) in abundances (**a** & **b**) and turnover (**c** & **d**) of zooplankton communities over the course of the experiment. Treatment concentrations reported in the legend reflect nominal applications of eugenol (applied as freely dissolved active substance or via the sepiolite nanocarrier). Replacement and turnover are expressed as normalized dissimilarity coefficients, indicating the summed and scaled change in abundances/incidence across taxa calculated per replicate, for respective time points relative to pre-treatment conditions (-14 days). Replacement and turnover are decomposed into gains (*C*) and losses (*B*) and scaled from 0 to 1, with 0 denoting no change and 1 denoting maximum change. Net replacement/turnover rates (*C* - *B*) are scaled from −1 to 1, with −1 denoting maximum net negative replacement or turnover (i.e., losses), 0 denoting no net replacement or turnover (i.e., losses equaling gains), and 1 denoting maximum net positive replacement or turnover (i.e., gains). See SI Table 3 for the full output of statistical tests.

and statistically non-significant decreases in overall taxon richness relative to controls (Eugenol: $\chi^2_{(1)} = 2.76, p = 0.10$; Eugenol × Time: $\chi^2_{(1)} = 3.35$, $p = 0.07$), with differences being more pronounced at later sampling moments (SI Figure 6c). Similarly, total abundances of zooplankton in the highest eugenol treatments were lower than those in controls at later time points (Eugenol: $\chi^2_{(1)} = 0.19$, $p = 0.66$; Eugenol × Time: $\chi^2_{(1)} = 4.67, p = 0.03$), although differences in this regard were minor compared to the overall variation in abundances between replicates (SI Figure 6 d). Decreases in total zooplankton abundance were unaffected by the type of formulation via which eugenol was applied (SI Table 1).

Analysis of replacement rates demonstrated more clear differences between treatments and controls, illustrating that zooplankton communities that received eugenol treatments exhibited both diminished gains (Bray-Curtis - Eugenol: $\chi^2_{(1)} = 8.64$, $p = 3.3 \times 10^{-3}$) and exacerbated losses (Bray-Curtis - Eugenol: $\chi^2_{(1)} = 12.4$, $p = 4.0 \times 10^{-4}$) in abundances (Fig. 4 a). Collectively, this resulted in a concentration-dependent decrease in net replacement rates (Bray-Curtis - Eugenol: $\chi^2_{(1)} = 12.63, p = 3.8 \times 10^{-4}$; Fig. 4 b). In mesocosms where eugenol was applied as freely dissolved active substance, mean differences from controls (± propagated standard error) in 20 and 200 µg L^{-1} treatments in this regard were −19.4 ± 21.2 % and −27.6 ± 21.2 % (after 7 days), −4.3 ± 21.3 % and −33.1 ± 21.2 % (after 28 days), and −6.7 ± 26.5 % and −16.2 ± 14.2 % (after 49 days), respectively. In mesocosms where eugenol was applied via the nanocarrier-based formulation, respective differences in 20 and 200 µg L^{-1} treatments were −33.8 ± 25.8 % and −47.9 ± 22.0 % (after 7 days), −28.8 ± 21.5 % and −42.1 ± 21.1 % (after 28 days), and −3.5 ± 21.7 % and −39.1 ± 13.5 % (after 49 days). With exception of observations for the lowest treatment concentration at the last sampling moment, net replacement rates were therefore consistently more negative in mesocosms where eugenol was applied via the nanocarrier-based formulation, although this yielded no significant interaction effect in overall models (Bray-Curtis – Eugenol × Nanocarrier: $\chi^2_{(1)} = 0.76$, $p = 0.38$). Differences from controls in turnover rates were less pronounced than those observed for replacement rates, but nevertheless demonstrated an increase in losses in mesocosms that

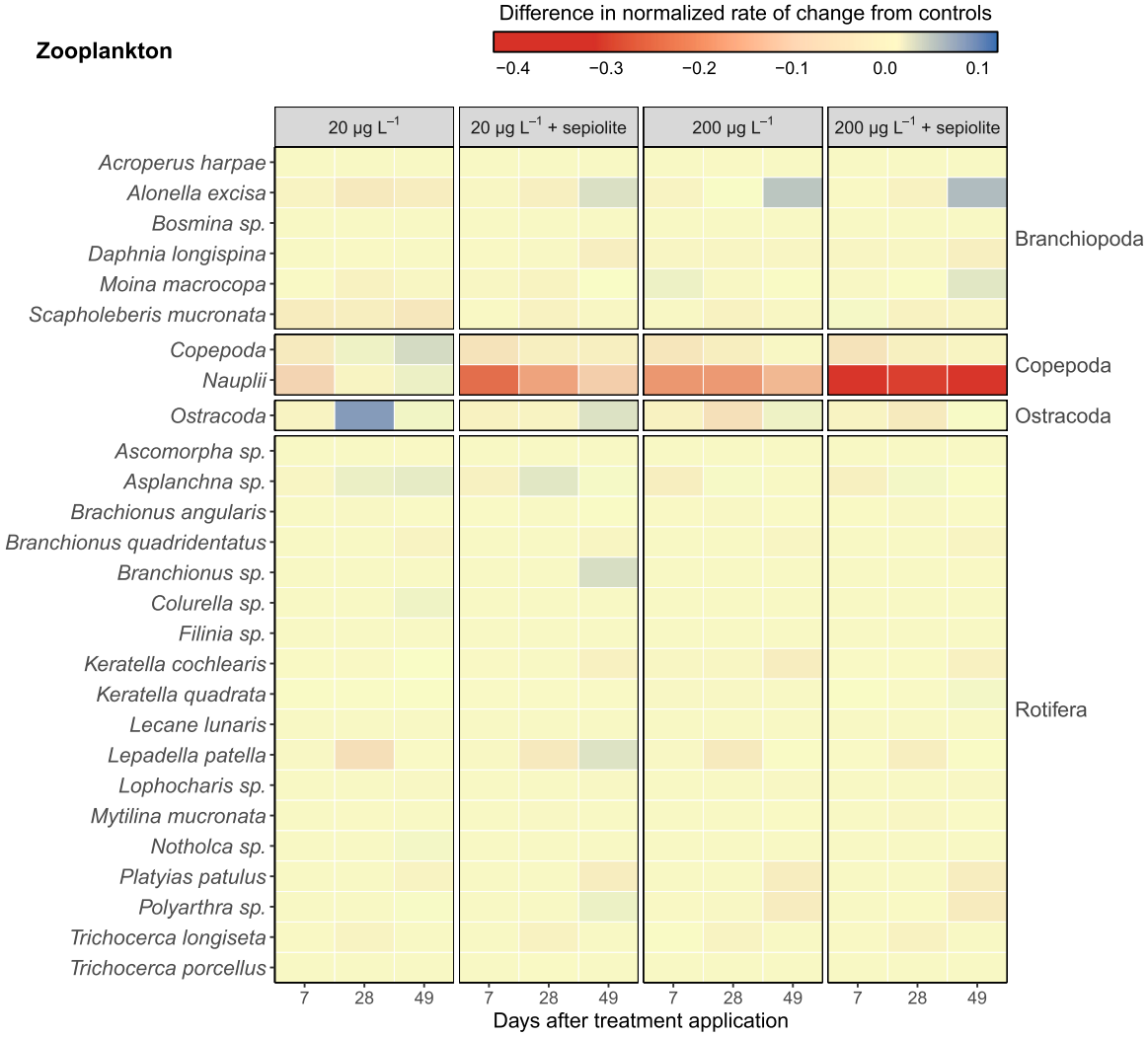

Fig. 5. Differences between treatments and controls in (mean) normalized rates of change in abundances of zooplankton over the course of the experiment. Treatment concentrations reflect nominal applications of eugenol (applied as freely dissolved active substance or via the sepiolite nanocarrier). Differences between treatments and controls are calculated based on the normalized net change in abundance (calculated per replicate) between respective time points and pre-treatment conditions (-14 days), which in turn is directly proportional to the contributions of individual taxa to temporal replacement in abundances at the community level (see Fig. 3 **a** & **b**). Positive differences in rates of change for a given treatment and time contrast denote that abundances of a taxon on average either increased more, or decreased less than in controls. Negative differences in rates of change in turn denote that abundances of a taxon either increased less, or decreased more than in controls. The limits of the color scale are adjusted to the minimum and maximum observed difference in rates of change across all comparisons. Taxa are clustered by Phylum/Class, i.e., Cladocera (water fleas), Copepoda (copepods, including nauplii), Ostracoda (ostracods), and Rotifera (rotifers). An equivalent overview based on presence-absence data (i.e., contributions to turnover rates) is provided in SI Figure 10.

received eugenol treatments (Sørensen - Eugenol: $\chi^2_{(1)} = 10.73$, $p = 1.1 \times 10^{-3}$). Here, effects manifested mostly in the higher treatment concentrations, regardless of the applied formulation, and remained of similar magnitude across all sampling moments (Fig. 4 c & d).

Losses in abundances and net negative replacement rates in mesocosms that received eugenol treatments were largely driven by nauplii (i.e., juvenile copepods), which decreased in numbers more steeply in response to higher treatment concentrations and as time progressed (Fig. 5). Interestingly, while adult copepods generally decreased in numbers in response to eugenol treatments as well, differences from controls in this regard were less pronounced than those for nauplii. This suggests that overall effects of eugenol on copepods mainly resulted from either reduced reproduction rates of adults, or from increased mortality rates in juveniles. Abundance shifts of taxa other than copepod nauplii showed considerably smaller differences from controls. In line with this, reanalysis of community-level replacement rates based on datasets from which nauplii were excluded showed that across other taxa, net replacement rates were only reduced in response to eugenol seven days after treatment application (Bray-Curtis – Eugenol: $F = 4.17$, $\chi^2_{(1)} = 8.35$, $p = 0.02$), with subsequent sampling moments after 28 (Bray-Curtis – Eugenol: $F = 0.46$, $\chi^2_{(1)} = 0.92$, $p = 0.63$) and 49 days (Bray-Curtis – Eugenol: $F = 0.47$, $\chi^2_{(1)} = 0.93$, $p = 0.63$) yielding no significant differences from controls. Similar to observations for macroinvertebrates, differences in turnover rates of zooplankton between treatments and controls were the results of comparatively small shifts in incidences across several taxa, with no apparent consistent responses in specific phyla or classes (SI Figure 10). As such, population and community-level impacts on zooplankton manifested mainly as decreases in abundances, rather than as full turnover in taxonomic composition, and were exacerbated and persisted over longer periods of time when eugenol was applied via the nanocarrier-based formulation.

3.2.3. *Emerging Insects - Abundances*

A total of 2550 arthropods were captured in emergence traps over the course of the experiment, with 288 specimens captured before treatment application, and 2262 after (SI Figure 5c). Insecta comprised the majority of specimens (98.8 % of totals), and Arachnida (exclusively Aranea - spiders) were encountered only sporadically (1.2 % of totals). Diptera (flies; 15 taxa) were the most abundant order among captured insects (84.0 % of totals), which in turn were dominated by non-biting (Chironomidae, comprising 72.6 % of all Diptera) and biting midges (Ceratopogonidae, comprising 20.4 % of all Diptera). Coleoptera (beetles; 6 taxa) and Ephemeroptera (mayflies; 1 taxon) made up 3.2 % and 2.3 % of the total collected specimens, respectively, and Odonata (exclusively Coenagrionidae - damselflies) Hemiptera (true bugs), Hymenoptera (exclusively Ichneumonidae - wasps), and Thysanoptera (thrips) all constituted less than 1 %. While Trichoptera (caddisflies) comprised 7.1 % of all collected arthropods, these were predominantly derived from a single species (Agraylea multipunctata) which was highly abundant in one replicate, but showed minimal occurrences in others. The distribution of biomass across arthropod orders differed from observations of relative abundances, with Diptera contributing the most to the total collected biomass (40.3 %), followed by Ephemeroptera (22.6 %), Coleoptera (21.1 %), and Odonata (14.3 % of totals). Here, a higher relative biomass of the latter orders (i.e., compared relative abundances) can be attributed to respective specimens generally exhibiting a several-fold higher biomass than specimens of Diptera. No differences in overall emergence rates ($F_{(25,4)} = 1.69$, $p = 0.18$) were observed prior to treatment application, but a slightly higher taxon richness was observed in samples from controls and mesocosms that received the highest treatment concentration of eugenol (200 μg L^{-1}) in nanocarrier treatments ($\chi^2_{(4)} = 10.97$, $p = 0.02$; SI Figure 6 e & f).

When summed across all taxa, insect emergence rates from mesocosms that received eugenol treatments were lower than those from controls (Fig. 6 a & b). Differences in this regard were most pronounced when eugenol was applied via the nanocarrier-based formulation (Eugenol × Nanocarrier × Time: $\chi^2 = 273.46$, $p = 0.03$), where nominal treatment concentrations of 20 and 200 μg L^{-1} resulted in overall reductions in cumulative abundances of 47.4 ± 12.6 % and 33.1 ± 18.8 %, respectively (mean ± propagated standard error). Differences from controls in mesocosms where eugenol was applied in its freely dissolved form were less pronounced (Eugenol × No nanocarrier × Time: $\chi^2 < 0.01$, $p = 0.89$), but in contrast to those in the nanocarrier treatments, did exhibit a slight dose-dependency, with total reductions in cumulative abundances amounting to 5.9 ± 19.3 % in 20 μg L^{-1} treatments, and 22.9 ± 16.1 % in 200 μg L^{-1} treatments. Notably, whereas emergence rates in treatments where eugenol was applied in its freely dissolved form gradually approached those in controls as time progressed, relative reductions from controls in treatments where eugenol was applied via the nanocarrier-based formulation grew more pronounced over time, indicating that the nanocarrier-based formulation both exacerbated and extended overall responses to eugenol in insect emergence rates.

Patterns observed for overall emergence rates were predominantly driven by contributions of specimens within the family Chironomidae (Diptera), which was the most abundant taxonomic group observed in emergence traps over the course of the experiment, and which showed responses to eugenol that were directionally equivalent but more distinct than those observed for emergence rates of all taxa combined (Fig. 6 c & d). Here as well, differences from controls were most evident in mesocosms where eugenol was applied via the nanocarrier-based formulation (Eugenol × Nanocarrier × Time: $\chi^2 = 664.10$, $p = 9.6 \times 10^{-4}$), amounting to overall relative reductions in cumulative emergence rates of 57.3 ± 15.8 % in 20 μg L^{-1} treatments, and 47.4 ± 19.4 % in 200 μg L^{-1} treatments. Differences from controls were less evident in mesocosms where eugenol was applied in its freely dissolved form (Eugenol × No nanocarrier × Time: $\chi^2 = 30.05$, $p = 0.20$), with respective reductions from controls in 20 and 200 μg L^{-1} treatments of 14.0 ± 20.5 % and 31.8 ± 20.3 %. These trends were reflected in those of Chironomidae larvae in aquatic macroinvertebrate samples, which decreased in abundance in response to eugenol treatments, in particular in mesocosms where eugenol was applied via the nanocarrier-based formulation (Fig. 3).

Emergence rates of Ceratopogonidae, the second-most abundant family of Diptera in the experiment, showed an overall increase in response to eugenol treatments (Fig. 6 e & f). While differences from controls in this regard were most consistent over time in mesocosms where eugenol was applied via the nanocarrier-based formulation (Eugenol × Nanocarrier × Time: $\chi^2 = 3.29$, $p = 0.04$), these were only apparent at the 200 μg L^{-1} treatment concentration, which showed relative increases in overall emergence rates of 56.7 ± 51.3 %. In mesocosms where eugenol was applied in its freely dissolved form, relative increases in emergence rates of Ceratopogonidae were 43.3 ± 33.8 % in 20 μg L^{-1} treatments and 59.7 ± 36.5 % in 200 μg L^{-1} treatments. However, differences from controls in this case were less pronounced and more variable at earlier time points, resulting in overall models indicating no significant effects of eugenol on emergence rates of Ceratopogonidae when applied as freely dissolved active substance (Eugenol × No nanocarrier × Time: $\chi^2 < 0.01$, $p = 0.98$). In contrast to observations for Chironomidae, trends of emerging Ceratopogonidae were reflected less unequivocally in those of larval stages derived from aquatic macroinvertebrate samples, with Ceratopogonidae larvae in mesocosms receiving the highest treatment concentration via the nanocarrier-based formulation decreasing in abundance relative to controls, while adult life stages in emergence traps showed a parallel increase in abundances (Fig. 3). This suggests that in the case of Ceratopogonidae, decreases in abundances of larvae were at least partially attributable to a higher likelihood of successful development into imagines (i.e., adult life stages). While other families of Diptera were occasionally encountered in the emergence traps, their abundances were considered insufficient for deriving meaningful inferences of potential treatment effects (Fig. 6 g & h). The same holds for specimens of other

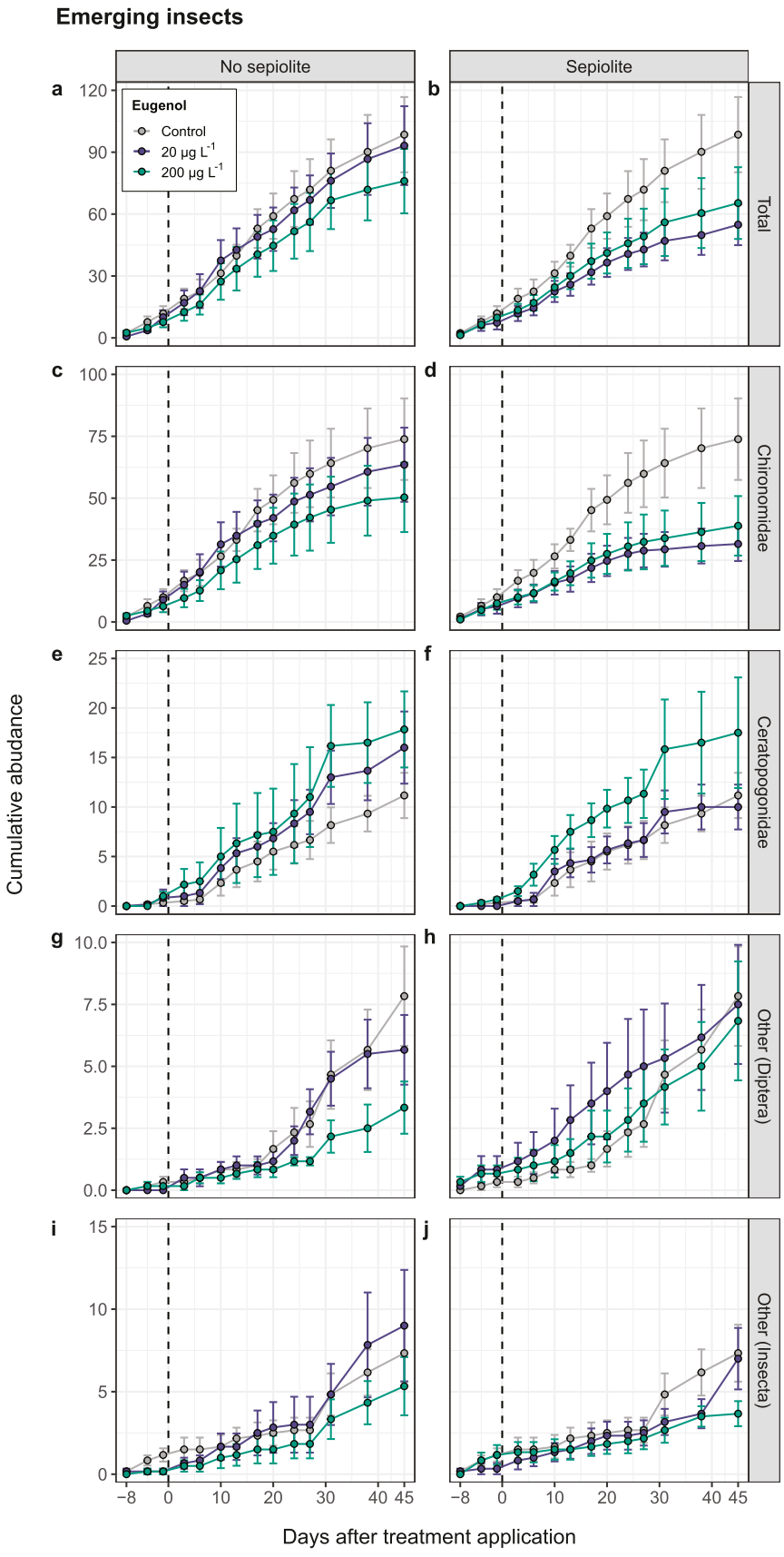

(caption on next page)

Fig. 6. Cumulative number (mean ± standard error, $n = 6$) of insects collected in emergence traps over the course of the experiment. Treatment concentrations reported in the legend reflect nominal applications of eugenol (applied as freely dissolved active substance or via the sepiolite nanocarrier). Trends are shown for the collective sum of all specimens (**a** & **b**), the sum of specimens from the most abundant families of Diptera (flies), i.e., Chironomidae (**c** & **d** - non-biting midges) and Ceratopogonidae (**e** & **f** - biting midges), the sum of specimens from other families of Diptera (**g** & **h** - including Cecidomyiidae, Chaoboridae, Culicidae, Cylindrotomidae, Dixidae, Empididae, Ephydridae, Liimonidae, Lonchaeidae, Psychodidae, and Scenopinidae), and the sum of specimens from remaining orders of Insecta (**i** & **j**), i.e., Coleoptera (beetles), Odonata (exclusively Coenagrionidae - damselflies), Ephemeroptera (mayflies), Hemiptera (true bugs), Hymenoptera (exclusively Ichneumonidae - parasitoid wasps), and Thysanoptera (thrips). The dashed line indicates the moment of treatment application. See SI Table 4 for the full output of statistical tests.

orders of insects, of which analyses were therefore omitted from further interpretation (Fig. 6 i & j).

Since larval stages of various species of both Chironomidae and Ceratopogonidae are known to feed on detritus and phytoplankton, it is conceivable that reductions in abundances of Chironomidae over the current experiment resulted in a decreased competitive pressure for acquiring resources for Ceratopogonidae [55,62]. At the same time, some species of Ceratopogonidae preferentially feed on small invertebrates, including the eggs and larvae of Chironomidae, as well as other macroinvertebrates and zooplankton [54,55]. Considering that abundances of Ceratopogonidae in the current experiment were too low to meaningfully analyze effects at a finer taxonomic resolution, the extent to which interactions such as these contributed to the directionality or magnitude of observed responses to eugenol treatments remains undetermined. Nevertheless, the findings from the current experiment do indicate that at the family level, Chironomidae are comparatively more sensitive to eugenol than Ceratopogonidae, and that furthermore, responses within both families were amplified when eugenol was applied via the nanocarrier-based formulation.

3.2.4. *Emerging insects - biomass*

Findings from overall biomass estimates in emergence traps showed similar trends to those of abundances, with the exception that here, relative reductions to controls were evident both for mesocosms that received eugenol via the nanocarrier-based formulation (Eugenol × Nanocarrier × Time: $F = 0.30$, $p = 7.5 \times 10^{-3}$) and for those that received eugenol in its freely dissolved form (Eugenol × Nanocarrier × Time: $F = 0.89$, $p = 1.6 \times 10^{-6}$; Fig. 7). Where eugenol was applied via

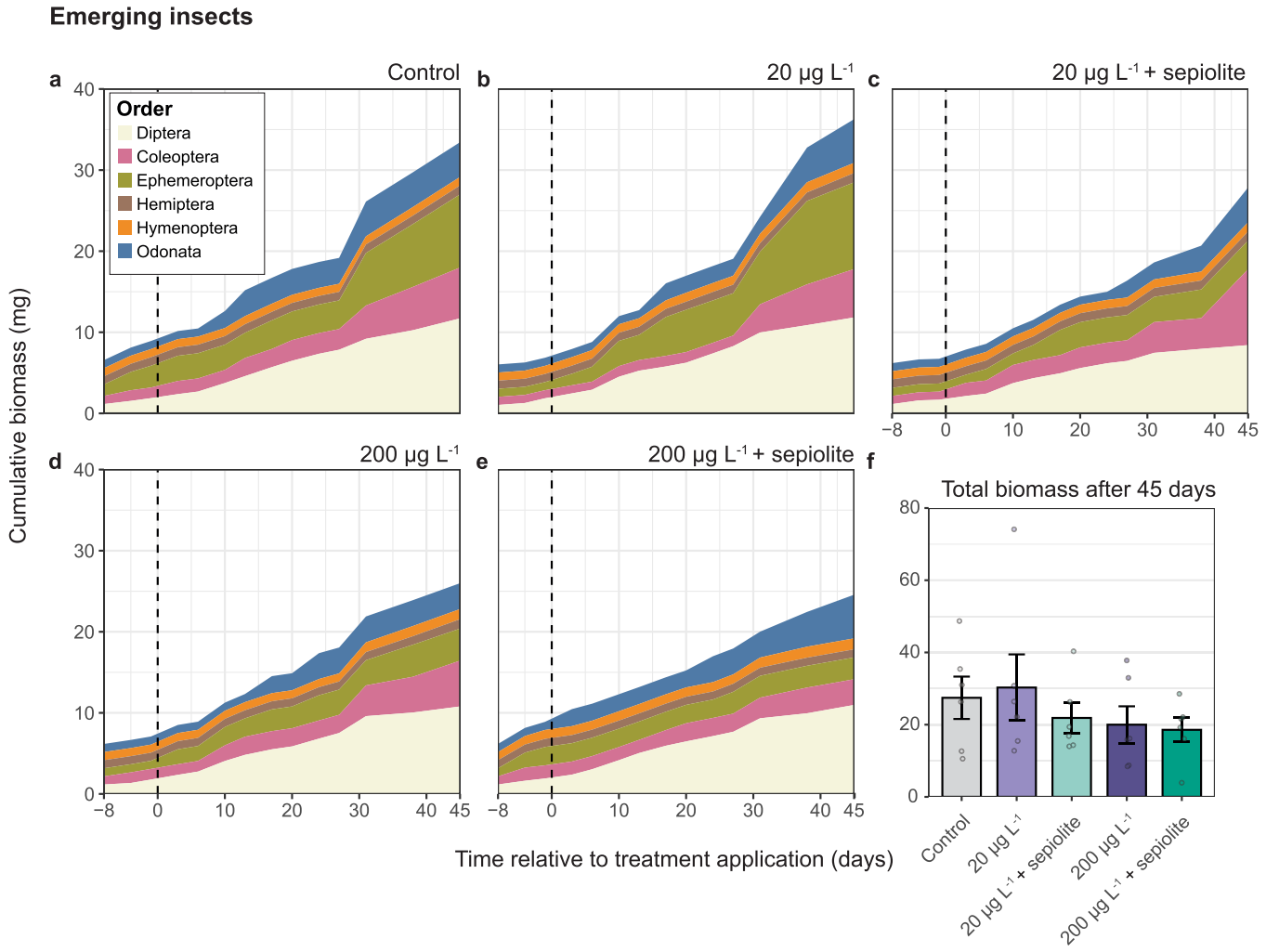

Fig. 7. Cumulative mean biomass ($n = 6$, dry weight) of the most abundant orders of insects collected in emergence traps over the course of the experiment (**a** - **e**), i.e., Diptera (flies), Coleoptera (beetles), Ephemeroptera (mayflies), Hemiptera (true bugs), Hymenoptera (exclusively Ichneumonidae - parasitoid wasps), and Odonata (exclusively Coenagrionidae - damselflies), and cumulative overall biomass (mean ± standard error, $n = 6$) at the end of the experiment (**f**). Treatment concentrations reflect nominal applications of eugenol (applied as freely dissolved active substance or via the sepiolite nanocarrier). The dashed line indicates the moment of treatment application. See SI Table 5 for the full output of statistical tests.

the nanocarrier-based formulation, reductions in cumulative insect biomass at nominal eugenol concentrations of 20 and 200 μg L^{-1} amounted to 20.3 ± 15.7 % and 32.3 ± 14.1 %, respectively. In mesocosms where eugenol was applied in its freely dissolved form, reductions were only apparent at the 200 μg L^{-1} treatment concentration (27.1 ± 19.4 %), with mesocosms receiving the 20 μg L^{-1} treatment concentration on average showing a slight increase (10.4 ± 33.5 %) in cumulative biomass relative to controls. In line with observations for abundances, reductions in biomass estimates could predominantly be ascribed to Diptera, where in turn, specimens within the family Chironomidae contributed to the largest extent (Eugenol × No nanocarrier × Time: F = 0.62, $p = 1.4 \times 10^{-4}$; Eugenol × Nanocarrier × Time: F = 2.59, $p < 2 \times 10^{-6}$). Other orders of insects however additionally showed an overall reduction in emerged biomass (Eugenol × No nanocarrier × Time: F = 0.71, $p = 2.9 \times 10^{-4}$; Eugenol × Nanocarrier × Time: F = 0.50, $p = 3.3 \times 10^{-3}$), which was predominantly due to a decrease in numbers of Ephemeroptera in both treatment concentrations where eugenol was applied via the nanocarrier-based formulation, and in the 200 μg L^{-1} treatment concentration where eugenol was applied in its freely dissolved form.

3.3. Nanocarrier-specific impacts on freshwater invertebrates

The findings from the current experiment illustrate that single applications of eugenol, at nominal treatment concentrations of both 20 and 200 μg L^{-1}, altered the temporal dynamics of non-target freshwater invertebrate populations and communities. Effects were most pronounced in zooplankton and emerging insects, and were characterized by a predominant decrease in abundances across various taxa relative to controls. Effects furthermore generally increased in magnitude along with increasing exposure concentrations, persisted throughout the 49-day experimental period, and were exacerbated when eugenol was applied via the nanocarrier-based formulation. A notable aspect in this regard is that freely dissolved eugenol concentrations in the experimental setup decreased to levels below the limit of detection within 48 h after application, regardless of the formulation via which eugenol was applied. As described previously, this is in concurrence with expectations regarding dissipation rates of eugenol in natural surface waters, which are likely to be high due to a combination of adsorption to organic matter, microbial and photodegradation, and volatilization [31]. However, the observed persistence of effects despite rapid dissipation of eugenol from the experimental systems suggests that either (1) short-term exposures to relatively high concentrations of eugenol, or (2) longer-term exposures to concentrations of eugenol below the detection limit of 1.07 μg L^{-1} in the current study, may have prolonged effects on population and community dynamics of freshwater invertebrates.

Toxicity data for eugenol in freshwater invertebrates are only scarcely available in the scientific literature and, to our knowledge, have largely been limited to laboratory-based assessments of acute effects on a small selection of crustaceans and insect larvae. Findings from such studies generally suggest that effect concentrations in aquatic invertebrates are one to several orders of magnitude higher than those at which long-term adverse effects were observed in the current experiment, with reported acute EC_{50}s for immobilization in *Daphnia magna* and *Daphnia pulex*, for example, ranging from 0.14 to 42.5 mg L^{-1} [38,40,41,56]. In larvae of the Dipteran species *Aedes aegypti* and *Ochlerotatus caspius*, both vectors of several of the major infectious diseases threatening human health around the globe, LC_{50}s for eugenol have been reported to range from 1.05 to 63.5 mg L^{-1}, and this has prompted several authors to propose its use as a larvicide for vector control [27,57,58]. The findings from the present study suggest that such applications are likely to also lead to longer-term impacts on non-target organisms occurring in treated waterbodies, and since this in turn could influence the development and reestablishment of vector populations (see e.g., Nelsen & Yee [59]), further evaluations to this end may be warranted prior to implementing the use of eugenol as a larvicide in vector control programs.

The observation from the current study that impacts of eugenol were more pronounced when application took place via the nanocarrier-based formulation points towards a modulating effect of the nanocarrier on the exposure dynamics and bioavailability of its active substance. Prolonged release profiles of eugenol from the nanocarriers at concentrations below the limit of detection may have contributed to this, and although the findings presented here provide no conclusive evidence to this end, extended exposure times have more frequently been noted as a point of concern with regard to non-target effects of nanocarrier-based formulations [15,21,22]. As such, extensive characterization of release profiles (and their potential dependency both environmental conditions and nanocarrier properties) may be considered a crucial aspect in further comparative studies into impacts of nanocarrier-based formulations and their active substances, and may help provide mechanistic insights that could benefit risk assessment practices.

One alternative factor that may have contributed to observations of differential impacts from the nanocarrier-based formulation and its freely dissolved active substance in the current experiment stems from exposure via ingestion. Filter- and deposit-feeding taxa in particular can be assumed to more effectively ingest nanocarrier-bound active substances, after which release from the nanocarrier may be accelerated in the digestive tract as a result of shifts in e.g., surrounding pH or ionic strength [60,61]. This mechanism has previously been proposed to explain exacerbated declines in population growth of *D. magna* following exposure to eugenol when applied via the same nanocarrier-based formulation as used in the current experiment [38]. Considering that Copepoda nauplii (i.e., juvenile Copepoda) and Chironomidae larvae, each feeding primarily on particulate matter, were amongst the most affected taxa in the current experiment, these findings highlight a need for further mechanistic evaluations into fate (i.e., in relation to suspension stability), exposure dynamics, and uptake routes of nanocarrier-bound substances, particularly in relation to ecological traits and feeding strategies of taxa of interest.

4. Outlook

Experimental assessments of non-target impacts of novel nanocarrier-based formulations of agrochemicals are still in their early stages, but from an environmental perspective may be considered a crucial element in weighing their favorability over that of conventional formulations currently in use. The present study demonstrates that higher-tier ecotoxicological approaches can effectively be tailored to this end, and provide sensitive and environmentally relevant estimates of comparative non-target impacts between nanocarrier-based products, formulations, and their active substances. It should however be noted that findings from case-studies such as those presented here are limited in their generalizability to other formulations and products, since the extent to which nanocarrier-based formulations may modulate non-target effects of their active substances may reasonably be expected to differ depending on interactions between their specific physical, chemical, and functional properties. Furthermore, it is worthwhile recognizing that when nanocarrier-based formulations function as intended, their ability to reduce application rates and limit the displacement of active substances to adjacent ecosystems could partially mitigate their overall non-target effects. We therefore emphasize that to meaningfully inform the development and risk assessment of nanocarrier-based formulations of agrochemicals, experimental evaluations of non-target effects should be performed in direct comparison with those of their active substances or alternative formulations, and that when possible, such evaluations should incorporate considerations of realistic reductions in displacement rates to ecosystems and compartments of interest that may be achieved under actual application scenarios.

Environmental implication

This study provides experimental evidence that nanocarrier-based pesticide formulations may exacerbate the environmental impacts of their active substances. In outdoor freshwater mesocosms, a eugenol-loaded nanocarrier formulation caused stronger and more persistent effects on invertebrate communities than its active substance (eugenol) alone. These findings suggest that nanocarriers can alter exposure pathways and prolong bioavailability, potentially increasing risks to non-target organisms. We pose that as the use of nanocarrier-based agrochemicals expands, such effects should be explicitly considered in environmental risk assessments. Our results highlight the need for comparative testing of nanocarrier-based formulations of agrochemicals under realistic exposure conditions to ensure that their claimed environmental benefits do not mask unintended ecological trade-offs.

CRediT authorship contribution statement

Tom A.P. Nederstigt: Writing – original draft, Methodology, Investigation, Formal analysis, Conceptualization. **Victor N. Huijer:** Writing – review & editing, Investigation. **Dennis Planjer:** Writing – review & editing, Investigation. **Felice J.M. Eekhout:** Writing – review & editing, Investigation. **S. Henrik Barmentlo:** Writing – review & editing, Investigation, Conceptualization. **Willie J.G.M. Peijnenburg:** Writing – review & editing, Conceptualization. **Martina G. Vijver:** Writing – review & editing, Funding acquisition, Conceptualization.

Acknowledgments

We are grateful to all volunteers, colleagues, and students who assisted throughout the experiment. In particular, we thank Bo Bode for his continuous support, Giovanni Ramanand for conducting the analytical determinations of eugenol, and Gerda Lamers, Sam Houdijk, and Pelle Wattel for collecting the electron microscopy micrographs of the nanocarriers. We are furthermore grateful for the efforts of Josephine Ligthart and Roemer Schoorl, who assisted during their BSc. internships, and Bregje Brinkmann, Lan Dupuis, and Martin van der Plas, who all provided valuable feedback throughout the study. The clove-oil loaded nanocarriers used in the experiment were provided by Encapsulae SL (Castellón de la Plana, Spain) as part of the European Union's Horizon 2020 SUNSHINE project (grant agreement number 952924), which additionally supported Willie J.G.M Peijnenburg. The facility maintenance and support for the presented work was funded by the *Campusregeling* of the province of South Holland. Tom A.P. Nederstigt and Martina G. Vijver received funding from the European Union's ERC-consolidator grant EcoWizard (grant agreement number 101002123).

Declaration of Competing Interest

The authors declare that they have no known competing financial interests or personal relationships that could have appeared to influence the work reported in this paper.

Appendix A. Supporting information

Supplementary data associated with this article can be found in the online version at doi:10.1016/j.jhazmat.2025.139560.

Data availability

The data that support the findings of this study are available via Dryad: http://doi.org/10.5061/dryad.k3j9kd5mz.

References

[1] Majumder, J., Taratula, O., Minko, T., 2019. Nanocarrier-based systems for targeted and site specific therapeutic delivery. Adv Drug Deliv Rev 144, 57–77. https://doi.org/10.1016/j.addr.2019.07.010.
[2] Scicluna, M.C., Vella-Zarb, L., 2020. Evolution of nanocarrier drug-delivery systems and recent advancements in covalent organic framework–drug systems. ACS Appl Nano Mater 3 (4), 3097–3115. https://doi.org/10.1021/acsanm.9b02603.
[3] Wang, D., Saleh, N.B., Byro, A., Zepp, R., Sahle-Demessie, E., Luxton, T.P., et al., 2022. Nano-Enabled pesticides for sustainable agriculture and global food security. Nat Nanotechnol 17 (4), 347–360. https://doi.org/10.1038/s41565-022-01082-8.
[4] Kah, M., Sabliov, C., Wang, Y., White, J.C., 2023. Nanotechnology as a foundational tool to combat global food insecurity. One Earth 6 (7), 772–775. https://doi.org/10.1016/j.oneear.2023.06.011.
[5] Vu Thanh, C., Gooding, J.J., Kah, M., 2025. Learning lessons from nano-medicine to improve the design and performances of nano-agrochemicals. Nat Commun 16 (1), 2306. https://doi.org/10.1038/s41467-025-57650-8.
[6] Hofmann, T., Lowry, G.V., Ghoshal, S., Tufenkji, N., Brambilla, D., Dutcher, J.R., et al., 2020. Technology readiness and overcoming barriers to sustainably implement nanotechnology-enabled plant agriculture. Nat Food 1 (7), 416–425. https://doi.org/10.1038/s43016-020-0110-1.
[7] Santos, P.A., Biraku, X., Nielsen, E., Ozketen, A.C., Ozketen, A.A., Hakki, E.E., 2025. Agricultural nanotechnology for a safe and sustainable future: current status, challenges, and beyond. J Sci Food Agric 105 (6), 3159–3169. https://doi.org/10.1002/jsfa.13922.
[8] Gressler, S., Hipfinger, C., Part, F., Pavlicek, A., Zafiu, C., Giese, B., 2025. A systematic review of nanocarriers used in Medicine and beyond — definition and categorization framework. J Nanobiotechnol. 23 (1), 90. https://doi.org/10.1186/s12951-025-03113-7.
[9] Organisation for Economic Co-operation (OECD). Development *Advanced Materials: Working Description*; OECD Series on the Safety of Manufactured Nanomaterials and Other Advanced Materials 2023 doi: 10.1787/4b5ba38d-en.
[10] Chariou, P.L., Ortega-Rivera, O.A., Steinmetz, N.F., 2020. Nanocarriers for the delivery of medical, veterinary, and agricultural active ingredients. ACS Nano 14 (3), 2678–2701. https://doi.org/10.1021/acsnano.0c00173.
[11] Wang, D., White, J.C., 2022. Benefit of nano-enabled agrochemicals. Nat Food 3 (12), 983–984. https://doi.org/10.1038/s43016-022-00665-x.
[12] Isman, M.B., 2020. Commercial development of plant essential oils and their constituents as active ingredients in bioinsecticides. Phytochem Rev 19 (2), 235–241. https://doi.org/10.1007/s11101-019-09653-9.
[13] Ferraz, C.A., Pastorinho, M.R., Palmeira-de-Oliveira, A., Sousa, A.C.A., 2022. Ecotoxicity of plant extracts and essential oils: a review. Environ Pollut 292, 118319. https://doi.org/10.1016/j.envpol.2021.118319.
[14] Farina, P., Conti, B., 2024. Liabilities of essential oils as insect repellents. Curr Opin Environ Sci Health 40, 100564. https://doi.org/10.1016/j.coesh.2024.100564.
[15] Grillo, R., Fraceto, L.F., Amorim, M.J.B., Scott-Fordsmand, J.J., Schoonjans, R., Chaudhry, Q., 2021. Ecotoxicological and regulatory aspects of environmental sustainability of nanopesticides. J Hazard Mater 404, 124148. https://doi.org/10.1016/j.jhazmat.2020.124148.
[16] Zhang, T., Sun, H., Hu, S., Ding, S., Zhang, P., Wang, L., et al., 2023. Self-Assembly of Eugenol-Loaded particles to regulate the adhesion of carriers on leaves for efficient foliar applications and ecotoxicological safety. Ecotoxicol Environ Saf 267, 115602. https://doi.org/10.1016/j.ecoenv.2023.115602.
[17] Pontes, M.S., Antunes, D.R., Oliveira, I.P., Forini, M.M.L., Santos, J.S., Arruda, G.J., et al., 2021. Chitosan/Tripolyphosphate nanoformulation carrying paraquat: insights on its enhanced herbicidal activity. Environ Sci Nano 8 (5), 1336–1351. https://doi.org/10.1039/D0EN01128B.
[18] Kah, M., Kookana, R.S., Gogos, A., Bucheli, T.D., 2018. A critical evaluation of nanopesticides and nanofertilizers against their conventional analogues. Nat Nanotechnol 13 (8), 677–684. https://doi.org/10.1038/s41565-018-0131-1.
[19] Yao, P., Zou, A., Tian, Z., Meng, W., Fang, X., Wu, T., et al., 2021. Construction and characterization of a temperature-responsive nanocarrier for imidacloprid based on mesoporous silica nanoparticles. Colloids Surf B Biointerfaces 198, 111464. https://doi.org/10.1016/j.colsurfb.2020.111464.
[20] Zhang, Y., Goss, G.G., 2022. Nanotechnology in agriculture: comparison of the toxicity between conventional and Nano-Based agrochemicals on Non-Target aquatic species. J Hazard Mater 439, 129559. https://doi.org/10.1016/j.jhazmat.2022.129559.
[21] Nederstigt, T.A.P., Brinkmann, B.W., Peijnenburg, W.J.G.M., Vijver, M.G., 2024. Sustainability claims of nanoenabled pesticides require a more thorough evaluation. Environ Sci Technol 58 (5), 2163–2165. https://doi.org/10.1021/acs.est.3c10207.
[22] Kookana, R.S., Boxall, A.B.A., Reeves, P.T., Ashauer, R., Beulke, S., Chaudhry, Q., et al., 2014. Nanopesticides: guiding principles for regulatory evaluation of environmental risks. J Agric Food Chem 62 (19), 4227–4240. https://doi.org/10.1021/jf500232f.
[23] Kah, M., 2015. Nanopesticides and nanofertilizers: emerging contaminants or opportunities for risk mitigation? Front Chem 3. https://doi.org/10.3389/fchem.2015.00064.
[24] Nederstigt, T.A.P., Peijnenburg, W.J.G.M., Schrama, M., Van Ommen, J.R., Vijver, M.G., 2022. Impacts of a novel Controlled-Release TiO2-Coated (Nano-) formulation of carbendazim and its constituents on freshwater macroinvertebrate communities. Sci Total Environ 838, 156554. https://doi.org/10.1016/j.scitotenv.2022.156554.

[25] Nederstigt, T.A.P., Bode, B., Van Ommen, J.R., Peijnenburg, W.J.G.M., Vijver, M. G., 2023. Zooplankton community turnover in response to a novel TiO2-Coated Nano-Formulation of carbendazim and its constituents. Environ Pollut 333, 121894. https://doi.org/10.1016/j.envpol.2023.121894.

[26] Forest, V., Pourchez, J., Flahaut, E., 2025. Efficiency and safety of nanopesticides, it takes two to tango. An overview of the lack of data on possible effects on human health. Sci Total Environ 973, 179156. https://doi.org/10.1016/j.scitotenv.2025.179156.

[27] Adhikari, K., Khanikor, B., Sarma, R., 2022. Persistent susceptibility of aedes aegypti to eugenol. Sci Rep 12 (1), 2277. https://doi.org/10.1038/s41598-022-06302-8.

[28] Zuo, J., Lan, R., Lv, N., Lin, Y., Hao, L., Zhou, X., et al., 2024. A promising Plant-Based Eugenol-Loaded nano delivery system (EUG@CMC-PGMA-CS) for enhanced antibacterial and insect repellent behavior. ACS Appl Bio Mater 7 (3), 1643–1655. https://doi.org/10.1021/acsabm.3c01100.

[29] Linda, C., Eleonora, G., Loretta, G., Priscilla, F., Camilla, T., Barbara, C., et al., 2025. Ecotoxicological assessment of basil essential oil on soil nematode communities. Environ Pollut 370, 125898. https://doi.org/10.1016/j.envpol.2025.125898.

[30] European Commission, (EC).). Commission Implementing Regulation (EU) 2021/1165 of 15 July 2021 Authorising Certain Products and Substances for Use in Organic Production and Establishing Their Lists.; Official Journal of the European Union; 2021. https://eur-lex.europa.eu/legal-content/EN/TXT/HTML/?uri=CELEX:02021R1165–20231115 (accessed 2025–05-10).

[31] Arena, M., Auteri, D., Leite, S.B., Binaglia, M., European Food Safety Authority (E. F.S.A.), 2024. Peer Review of the Pesticide Risk Assessment of the Active Substance Clove Oil. EFSA J (4), 22. https://doi.org/10.2903/j.efsa.2024.8671.

[32] Lagaly, G., 2001. Pesticide–Clay interactions and formulations. Appl Clay Sci 18 (5–6), 205–209. https://doi.org/10.1016/s0169-1317(01)00043-6.

[33] Shaltiel-Harpaz, L., Kreimer, T., Dudai, N., Kaspi, R., Ben-Yakir, D., Rytwo, G., 2023. Sepiolite- rosemary oil combination as an environmentally oriented insecticide. Appl Clay Sci 234, 106838. https://doi.org/10.1016/j.clay.2023.106838.

[34] Maqueda, C., Partal, P., Villaverde, J., Perez-Rodriguez, J.L., 2009. Characterization of Sepiolite-Gel-Based formulations for controlled release of pesticides. Appl Clay Sci 46 (3), 289–295. https://doi.org/10.1016/j.clay.2009.08.019.

[35] Casal, B., Merino, J., Serratosa, J.-M., Ruiz-Hitzky, E., 2001. Sepiolite-based materials for the photo- and thermal-stabilization of pesticides. Appl Clay Sci 18 (5–6), 245–254. https://doi.org/10.1016/s0169-1317(01)00030-8.

[36] Del Carmen Galán-Jiménez, M., Morillo, E., Bonnemoy, F., Mallet, C., Undabeytia, T., 2020. A Sepiolite-Based formulation for slow release of the herbicide mesotrione. Appl Clay Sci 189, 105503. https://doi.org/10.1016/j.clay.2020.105503.

[37] Yalkowsky, S.H., He, Y., Jain, P., 2010. Handbook of aqueous solubility data: an extensive compilation of aqueous solubility data for organic compounds extracted from the AQUASOL dATAbASE. CRC Press LLC, Boca Raton, Florida, USA.

[38] Brinkmann, B.W., Dupuis, L., Houdijk, S., Wattel, P., Salgado, C., Brunelli, A., et al., 2025. Eugenol-loaded nanocarriers exert Particle-Specific adverse effects to daphnia magna populations. Environ Sci Technol 59 (31), 16293–16303. https://doi.org/10.1021/acs.est.5c03624.

[39] Pizzol, L., Livieri, A., Salieri, B., Farcal, L., Soeteman-Hernández, L.G., Rauscher, H., et al., 2023. Screening level approach to support companies in making safe and sustainable by design decisions at the early stages of innovation. Clean Environ Syst 10, 100132. https://doi.org/10.1016/j.cesys.2023.100132.

[40] Gueretz, J.S., Somensi, C.A., Martins, M.L., Souza, A.P.D., 2017. Evaluation of eugenol toxicity in bioassays with Test-Organisms. Ciênc Rural 47 (12). https://doi.org/10.1590/0103-8478cr20170194.

[41] European Chemicals Agency, (ECHA). ECHA REACH Registered Dossier. https://echa.europa.eu/cs/registration-dossier/-/registered-dossier/13694/1/1 (accessed 2025–05-10).

[42] Zink, L., Meslo, M., Wiseman, S., Pyle, G.G., 2024. *daphnia magna* digestive activity is differentially altered when exposed to equally turbid waters caused by either suspended sediment or suspended microplastics. Environ Toxicol 39 (4), 2086–2091. https://doi.org/10.1002/tox.24096.

[43] Robinson, S.E., Capper, N.A., Klaine, S.J., 2010. The effects of continuous and pulsed exposures of suspended clay on the survival, growth, and reproduction of *daphnia magna*. Environ Toxicol Chem 29 (1), 168–175. https://doi.org/10.1002/etc.4.

[44] Schneider, C.A., Rasband, W.S., Eliceiri, K.W., 2012. NIH image to ImageJ: 25 years of image analysis. Nat Methods 9 (7), 671–675. https://doi.org/10.1038/nmeth.2089.

[45] Floßner, D., 2000. *die haplopoda und cladocera (ohne bosminidae) mitteleuropas*; backhuys publishers. Kerkwerve, The Netherlands.

[46] Notenboom-Ram, E., 1989. Verspreiding en ecologie van de branchiopoda in nederland. RIN Rapport 91/14 Rijksinst voor Nat. RIN Rapport 91/14.

[47] Cadmus, P., Pomeranz, J.P.F., Kraus, J.M., 2016. Low-Cost floating emergence net and bottle trap: comparison of two designs. J Freshw Ecol 31 (4), 653–658. https://doi.org/10.1080/02705060.2016.1217944.

[48] Barmentlo, S.H., Schrama, M., De Snoo, G.R., Van Bodegom, P.M., Van Nieuwenhuijzen, A., Vijver, M.G., 2021. Experimental evidence for neonicotinoid driven decline in aquatic emerging insects. Proc Natl Acad Sci 118 (44), e2105692118. https://doi.org/10.1073/pnas.2105692118.

[49] Oosterbroek, P., 2012. De europese families van muggen en vliegen (Diptera). KNNV Publishing, Utrecht, The Netherlands.

[50] Anderson, M.J., Crist, T.O., Chase, J.M., Vellend, M., Inouye, B.D., Freestone, A.L., et al., 2011. Navigating the multiple meanings of β diversity: a roadmap for the practicing ecologist: roadmap for beta diversity. Ecol Lett 14 (1), 19–28. https://doi.org/10.1111/j.1461-0248.2010.01552.x.

[51] Legendre, P., 2019. A temporal Beta-diversity index to identify sites that have changed in exceptional ways in Space–Time surveys. Ecol Evol 9 (6), 3500–3514. https://doi.org/10.1002/ece3.4984.

[52] R. Core Team. R: A Language and Environment for Statistical Computing, 2025. ⟨https://www.R-project.org/⟩.

[53] Li, X., Tao, Y., Zhu, L., Ma, S., Luo, S., Zhao, Z., et al., 2022. Optical and chemical properties and oxidative potential of Aqueous-Phase products from OH and ^{3}C* -Initiated photooxidation of eugenol. Atmos Chem Phys 22 (11), 7793–7814. https://doi.org/10.5194/acp-22-7793-2022.

[54] Szadziewski, R.; Krzywinski, J.; Gilka, W. *Diptera Ceratopogonidae, Biting Midges*. In A. Nilsson (*Ed.), Aquatic Insects of North Europe: A Taxonomic Handbook*; 1997.

[55] Wagner, R., Barták, M., Borkent, A., Courtney, G., Goddeeris, B., Haenni, J.-P., et al., 2008. Global diversity of dipteran families (Insecta Diptera) in freshwater (Excluding Simulidae, Culicidae, Chironomidae, Tipulidae and Tabanidae). Hydrobiologia 940 (1), 489–519. https://doi.org/10.1007/s10750-007-9127-9.

[56] Sutili, F.J., Gressler, L.T., Baldisserotto, B., 2014. Anthelmintic activity of the phytochemical eugenol against the fish parasite gyrodactylus sp. And acute toxicity in daphnia pulex. PanAm J Aquat Sci 9 (3), 223–227.

[57] Hribar, L.J., Murray, H.L., 2019. Toxicity of naled and eugenol to mosquito larvae, 2018. Arthropod Manag Tests 44 (1). https://doi.org/10.1093/amt/tsz016.

[58] Subahar, R., Huang, A., Wijaya, R.S., Nur, L.S.E., Susanto, L., Firmansyah, N.E., et al., 2024. First report on evaluation of commercial eugenol and piperine against aedes aegypti l (Diptera: Culicidae) larvae: mortality, detoxifying enzyme, and histopathological changes in the midgut. Parasitol Int 98, 102813. https://doi.org/10.1016/j.parint.2023.102813.

[59] Nelsen, J., Yee, D.A., 2023. Non-Target effects of methoprene and larvicidal surface films on invertebrate predators of mosquito larvae. J Vector Ecol 48 (1). https://doi.org/10.52707/1081-1710-48.1.41.

[60] Slattery, M., Harper, B., Harper, S., 2019. Pesticide encapsulation at the nanoscale drives changes to the hydrophobic partitioning and toxicity of an active ingredient. Nanomaterials 9 (1), 81. https://doi.org/10.3390/nano9010081.

[61] Wu, F., Zhang, S., Li, H., Liu, P., Su, H., Zhang, Y., et al., 2024. Toxicokinetics explain differential freshwater ecotoxicity of nanoencapsulated imidacloprid compared to its conventional active ingredient. Environ Sci Technol 58 (22), 9548–9558. https://doi.org/10.1021/acs.est.4c00065.

[62] Hayford, B.L., Sublette, J.E., Herrmann, S.J., 1995. Distribution of Chironomids (Diptera: Chironomidae) and Ceratopogonids (Diptera: Ceratopogonidae) along a Colorado Thermal Spring Effluent. J. Kans. Entomol. Soc. 77–92. https://www.jstor.org/stable/25085635.